ELSEVIER

Contents lists available at ScienceDirect

Journal of Molecular Liquids

journal homepage: www.elsevier.com/locate/molliq



Physicochemical properties of deep eutectic solvent choline chloride: Propionic acid (ChCl/PA DES) and its binary solutions with 1-butanol as cosolvent

Aafia Sheikh^{a,*}, Ariel Hernández^{b,**}, Athar Yaseen Khan^c, Safeer Ahmed^d

- ^a Department of Chemistry, Government College Women University, Sialkot, Pakistan
- b Departamento de Ingeniería Industrial, Facultad de Ingeniería, Universidad Católica de la Santísima Concepción, Alonso de Ribera 2850, Concepción, Chile
- c Department of Chemistry, Forman Christian College (A Chartered University), Lahore, Pakistan
- ^d Department of Chemistry, Quaid-i-Azam University, Islamabad, Pakistan

ARTICLE INFO

Keywords: Physicochemical properties Redlich-Kister polynomial equation Perturbed chain statistical associating fluid theory Schaaff's collision factor theory Nomoto relation Free volume theory

ABSTRACT

Deep eutectic solvents (DESs) are considered suitable replacement for conventional organic solvents, and the prospects of their use in pharmaceutical and biomedical fields are growing. A detailed knowledge of their physicochemical properties and understanding about structural behavior are particularly important for academic and industrial applications. In the present study a deep eutectic solvent is prepared by combination of choline chloride (ChCl) and propionic acid (PA) designated as ChCl/PA DES. Physicochemical properties density (ρ) , speed of sound (u) and dynamic viscosity (η) of ChCl/PA DES and its binary mixtures with cosolvent n-butanol are measured in the temperature range (293.15 – 333.15) K for all compositions $x_1 = 0 - 1$ (x_1 is mole fraction of ChCl/PA DES). The density data is appropriately fitted with a second-degree polynomial equation in T. The volumetric properties, excess molar volume (V^E) and isentropic compressibility deviation ($\Delta \kappa_S$), of ChCl/PA DES and its binary solutions show negative deviation from ideal behavior. The V^E vs x_1 curves exhibit a minimum at $x_1 \approx 0.35$ which becomes deeper with increasing T. Curves corresponding to excess partial molar volume of the DES and 1-Butanol also cross each other at $x_1 \approx 0.35$ which supports dominance of packing effect over specific interactions. Similar behavior in viscosity deviation ($\Delta \eta$) is also observed but at $x_1 \approx 0.6$ which is again supportive of the volumetric results. Lattice energy (U_{pot}) , molar entropy (S^0) and intermolecular free length (L_f) are calculated to explore behavior of the derived thermodynamic properties. Comparison of the results of temperature dependence of transport property (η) with Vogel Fulcher Tammann (VFT) and Arrhenius equations reveals that the VFT equation satisfactorily explains the relationship between dynamic viscosity and T. To model the properties, we treat DES as a pseudo pure fluid and the DES + 1-butanol mixture as a pseudo binary system. The Perturbed Chain Statistical Associating Fluid Theory (PC-SAFT) equation of state was employed as a fitting approach for modeling the experimental density of ChCl/PA DES + 1-butanol mixtures. The theoretical models named Schaaff's Collision Factor Theory (SCFT) and Nomoto's Relation (NR) were used to compute the speed of sound (u) for the mixtures from theoretical point of view. Finally, dynamic viscosity (η) was modeled using Free Volume Theory (FVT). This theory was applied as a fitted method using only three fitted parameters across the entire range of temperature and liquid mole fraction of DES.

1. Introduction

Organic solvents are generally used in chemical industry and in many other application where they are required. Hazardous nature of these solvents has presented a threat to our environment and quality of life. Hence presently there is great emphasis to replace them with environmentally friendly solvents as a matter of commitment to fulfil the objectives of green chemistry practice [1]. In this effort a step towards this goal materialized in the synthesis of ionic liquids (ILs) which were salts whose melting points were below 100 °C and composed of an

E-mail addresses: aafia.sheikh@gcwus.edu.pk (A. Sheikh), ahernandez@ucsc.cl (A. Hernández).

https://doi.org/10.1016/j.molliq.2025.127217

^{*} Corresponding author at: Department of Chemistry, Government College Women University, Sialkot 51310, Pakistan.

^{**} Corresponding author.

inorganic anion and an organic cation.

Their characteristic properties such as high thermal stability, low vapor pressure, broad liquid range and low melting point (<100 °C) were attractive for applications in research, chemical industry and engineering processes [2]. However, cumbersome and time consuming procedure involved in synthesizing pure samples, expensive starting materials and toxicity profile of the product were impediments in their further development and application as an alternate solvent medium [3]. Next deep eutectic solvents (DESs) were prepared as a eutectic mixtures by combining a hydrogen bond donor (HBA) with a hydrogen bond acceptor (HBA). They exhibited desirabale physicochemical properties like low vapor pressure, low melting points and others comparable with ILs but cheaper in cost and easy to prepare. DESs are considered as promising green alternative for ILs and conventional organic solvents. The search for new and alternative green solvents with excellent physicochemical properties have led to the preparation of deep eutectic solvents. By carefully choosing constituents from a huge store of HBAs and HBDs, a structure based DES can be prepared which is biodegradable with low toxicity profile. The constituents for Natural deep eutectic solvents (NADES) are precursors which are metabolites of biological significance such as sugars, polyols, amino acids and choline derivatives. NADES formed from them are suitable for pharmaceutical and biomedical application due to better biodegradability, sustainability and low toxicity [4].

The two components involved in the formation of DESs could be liquids, solids, ions, or neutral molecules. The hydrogen bond formation and the charge delocalization between participating HBA and HBD hinders the crystallization of the individual components [5]. The term "deep" signifies the negative temperature deviation at the eutectic point compared to the predicted temperature for an ideal liquid mixture [6]. An added practical advantage of DESs is that unlike ILs, they require no additional exhaustive purification process after their formation [7]. In summary vesatile properties of DESs together with low production cost, and easy synthesis from readily available precursors makes them an excellent candidate to replace ILs and duly supports the green solvent tag attached to them. With the advent of DESs, use of ILs in pharmaceutical and biomedical industry and has been limited due to obvious reasons of toxicity, high production cost and low purity [8–10].

Choline chloride (also known as Vitamin B4) is a readily available, nontoxic and biodegradable quarternary ammonium salt which is produced at mass scale in the world. It is used as an additive in animal feed and also a commonly used HBA for preparing DESs [11]. Its low enthalpy of fusion (about 4.3 kJ.mol⁻¹) facilitates the melting temperature depression for DES formation [12].

Carboxylic acids (e.g., acetic acid, propionic acid and lactic acid, etc) are compounds which possess useful chemical properties for use in pharmaceutical industry. They are mostly sourced from acidogenic fermentation of organic matter and their pKa value (3.5-4.5) suggests that they are in the deprotonated state in biological media [13]. The organic acids based DESs are extensively used to enhance the dissolution of drugs in aqueous media [14,15].

In the present study, ChCl/PA DES is prepared from choline chloride (ChCl) and Propionic acid in the 1: 2 mol ratio for investigating its physicochemical properties (density, speed of sound and dynamic viscosity) and its binary solutions with 1-butanol.

Physicochemical properties of DESs are sensitive to presence of moisture in trace amounts as water breaks down the hydrogen bonded network of DES and forms new bonds with chloride anion or HBD [16–18]. There is a relationship between the chain length of carboxylic acid of DES and the rate and absorption capacity of water molecules [19,20].

DESs finds many targeted applications in electrochemistry, pharmaceutical formulation, colloidal chemistry, synthesis, catalysis, extraction and biodeisal purification [21–23]. The solubility of natural products is higher in DESs compared to conventional solvents due to the hydrogen bond formation with DESs. Use of ChCl/PA DES has beed

reported for extraction of phytochemical compounds and desulfurization of fuel (gasoline and diesel) [24,25]. Relatively higher viscosity of DESs and the lack of information on structure and properties could place some restriction on their use in many practical applications. Recent studies show that the solubilization behavior of deep eutectic solvent (DES) is optimized by adding appropriate molecular solvent (for example, water, alcohols of diffent carbon chain length and DMSO) and composition variation of mixtures for engineering applications [26,27]. Moreover, the mass transfer of bioactive molecules from natural matrices is improved with addition of cosolvent [28].

Targeted applications of DES and its mixtures with cosolvent(s) require knowledge of physicochemical properties of solution system and understanding of the microscopic interactions present within it [29]. There is no established theory based entirely on HBA and HBD chemistry which explains the tailoring and tuning of physicochemical properties. Properties of binary mixtures of DESs with alcohols are of interest for their uses in pharmaceutical, cosmetic industry, organic synthesis, separation processes, and battery technology [30-32]. The presence of -OH group in alcohol molecule imparts strong dependence of the system on hydrogen bonding [33]. 1-Butanol is a versatile chemical platform commonly used as food extractant, plasticizer, binder, in paint and plastic industry. It has also been considered as an excellent alternative to conventional fuels diesel and gasoline [34]. The long hydrocarbon chain, lower vapor pressure, and non-polar characteristic of 1-butanol are its advantageous characteristics for use as cosolvent compared to ethanol [35,36]. 1-Butanol is often produced from biomass, called "biobutanol" and from fossil fuels called "petrobutanol", both forms having the same chemical properties. The knowledge of thermophysical properties DES is essentially important for technical applications in semiconductor industry and other industrial processes [37]. The significance of these properties relates to designing and optimization of industrial process equipment and ensuring process quality for efficient operation of the industrial system [38]. Emission of CO₂ by industrial units, power plants and fuel based vehicles is a major source of pollution. Recently DES based CO2 capture technology has gained much attention due to higher absorption effeciency at relatively low cost [39]. Several publications have appeared in literature on DES/water mixtures but similar studies with 1-butanol are few [29,40,41].

The objective of the present study is (1) to prepare and characterize DES composed of choline chloride and propionic acid in (1:2) mole ratio and (2) to study the thermophysical (density, ρ and speed of sound, u) and transport property (dynamic viscosity, η) of binary mixtures of DES and1-butanol for all compositions in the range $x_1=0$ to 1 $(x_1$ is mole fraction of DES) and temperatures (293.15 - 333.15) K at ambient pressure. Volumeric and accoustic paramers are derived from regression analysis of the experimental data as a function of temperature and compositions. Functional dependence of experimental dynamic viscosity (η) on x_1 and T is satisfactorily fitted with Vogel Fulcher Tammann (VFT) equation.

For computational studies, the liquid density for the DES + 1-butanol mixture was determined through the application of the perturbed chain statistical associating fluid theory equation of state (PC-SAFT EoS) [42,43]. For modeling the speed of sound, two predictive methods were employed: PC-SAFT EoS combined with Schaaff's collision factor theory (SCFT) [44] and with Nomoto's relation (NR) [45]. To model the dynamic viscosity, the free volume theory (FVT) [46–48] was coupled to PC-SAFT EoS.

1.1. Materials

Details of chemicals used in this work are listed in Table 1 with their CAS numbers, source, and purity.

1.2. Methods

The ChCl/PA DES was prepared following the procedure already

Table 1
CAS registry number, source, and purity of the chemicals.

Chemical	CAS Reg. No.	Source	Purity	Purification method
Choline chloride	67-48-1	Sigma- Aldrich	≥99 %	Used as received
Propionic acid	79-09-4	Daejung	≥99 %	Used as received
1-Butanol	71-36-3	Sigma- Aldrich	≥99 %	Used as received

reported [14,49,50].

Choline chloride (HBA) and propionic acid (HBD) were mixed by adjusting 1:2 M ratio. The mixture was heated in a round bottom flask at (343.15 - 348.15) K with constant stirring. The flask was fitted with a condenser at the end of which a drying tube filled with silica gel was provided. The contents of the flask were continuously stirred until a homogeneous, colorless, and transparent liquid of ChCl/PA DES was formed. The prepared DES was allowed to cool to room temperature and stored in a sealed bottle and kept in a desiccator. The moisture content of the final product (ChCl/PA DES) was determined with coulometric Karl Fischer titration equipment (Mettler Toledo, V10S) using Karl Fischer reagent (CombiNorm5 and methanol) which was 0.05 %. To characterize the prepared ChCl/PA DES, FTIR spectra of choline chloride, ChCl/PA DES and propionic acid were recorded on FTIR spectrometer (ALPHA, Bruker II), and NMR (¹H and ¹³C) spectra were recorded on Bruker Advance 300 MHz spectrometer. These spectra are shown in Figs. S1–S3 (Supporting information).

Binary solutions of ChCl/PA DES and 1-butanol over the entire range of composition were prepared by weighing of components in airtight glass vials using analytical balance (Shimadzu AUW220D, precision \pm 0.01 mg).

The FTIR spectra of ChCl/PA DES and 1-butanol binary mixtures corresponding to mole fractions ($x_1 = 0.0, 0.3, 0.5, 0.7, 1.0$) have also been recorded and shown in Fig. S4 (Supporting information).

Density and speed of sound meter (DSA 5000 M, Anton Paar) was used for density (p) and speed of sound (u) measurements in (293.15 – 333.15) K temperature range at 5 K intervals. The instrument is equipped with density and speed of sound cell, combining oscillating U-tube method. Both cells were temperature controlled by built-in Peltier thermostat with an uncertainty of 0.01 K. The density was measured by vibrating tube densimeter. Density was derived from the resonant frequency of sample filled U-shaped tube as it vibrates perpendicular to its plane in an electromagnetic field. The vibration was considered as simple harmonic oscillation. The ultrasonic transducer frequency of DSA-5000 M was 3 MHz. The speed of the sound was derived by determining the period of received sound waves and by considering the distance between transmitter and receiver. Prior to each measurement, calibration of the instrument was checked with deionized water and air. The measuring tube of DSA 5000 was thoroughly cleaned with deionized water, rinsed with ethanol, and dried using a blower before injecting each sample.

Viscosity module (Lovis 2000 M/ME, Anton Paar) attached to DSA 5000 was used for viscosity measurements in temperature range (293.15 – 333.15) K. The dynamic viscosity (η) measurements are based on the falling ball principle. The falling time of a steel ball in the capillary tube filled with the sample fluid is measured. The stated temperature uncertainty and repeatability factor of DSA 5000 and the Module 2000 were 0.01 K, 0.02 K, 0.01 K, and 0.005 K, respectively. Viscosity measurements were made with capillary tubes of diameter 1.59, 1.8 and 2.5 mm, respectively which were calibrated at different temperatures and angle inclinations, with viscosity standards (S3, S6, N100 and N415) supplied by Anton Paar. The standard uncertainties in mole fractions, density, speed of sound and dynamic viscosity were $u(x_1) = 0.01$, u(T) = 0.01 (for density), $u(\rho) = 3 \times 10^{-3} \ kg.m^{-3}$, $u(u) = 0.50 \ m.s^{-1}$ u(T) = 0.02 (for viscosity) and $u(\eta) = 0.01 \ mPa.S$, respectively using

Eqs. S9–S12 (Supporting information).

2. Computational modeling

2.1. Liquid density using PC-SAFT EoS

According to the literature, density modeling for mixtures with DES has been successfully applied with PC-SAFT [51–54]. This theoretical model states that the liquid density can be calculated with Eq. (1):

$$\left[\rho\left(\frac{\partial a}{\partial \rho}\right)_{T,V} - a\right] = P \tag{1}$$

where T is the temperature, ρ indicates the molar density, V is the molar volume, and a=A/V represents the Helmholtz energy density, with A is the molar Helmholtz energy. According to this theoretical model, the Helmholtz energy density is defined as Eq. (2):

$$a = \rho(A^{ig} + A^{hc} + A^{disp} + A^{assoc})$$
 (2)

where A^{ig} , A^{hc} , A^{disp} , and A^{assoc} are related to ideal gas term, a hard-chain contribution, London forces, and association term, respectively. Given that equations related to contributions for molar Helmholtz energy are thoroughly documented in the literature, and to maintain focus on the key aspects of PC-SAFT EoS, readers are advised to refer to the cited sources [42,43].

Each pure fluid requires five fitted parameters: the segment diameter that does not vary with temperature (σ) , the number of segments (m), the energy parameter (ε) , the effective volume (κ^{AB}) , and the association energy parameter (ε^{AB}) . For pure fluids that do not exhibit self-association, the last two parameters are assigned a value of zero.

Once the pure fluid parameters are established, the appropriate mixing rules must be applied for the binary mixtures, i.e., the mixing rules expressed as Eqs. (3–6):

$$\varepsilon_{ij} = \sqrt{\varepsilon_i \varepsilon_j} (1 - k_{ij}) \tag{3}$$

$$\sigma_{ij} = \frac{1}{2} \left(\sigma_i + \sigma_j \right) \tag{4}$$

$$\varepsilon^{A_i B_j} = \frac{1}{2} \left(\varepsilon^{A_i B_i} + \varepsilon^{A_j B_j} \right) \tag{5}$$

$$\kappa^{A_i B_j} = \sqrt{\kappa^{A_i B_i} \kappa^{A_j B_j}} \left[\frac{\sqrt{\sigma_i \sigma_j}}{\left(\sigma_i + \sigma_j\right)/2} \right]^3 \tag{6}$$

Therefore, in the cross dispersive energy parameter (ε_{ij}) , the binary interaction parameter (k_{ij}) is present. This parameter is fitted to account for the attractive dispersion forces between molecules i-j. This binary parameter is usually fitted with phase equilibrium data, but in the absence of experimental phase equilibrium data and in order to better model the liquid density of the mixture, in this work it will be fitted with density data.

2.2. Speed of sound using SCFT and NR

In this study, two models were used to calculate the speed of sound: SCFT [44] and NR [45]. A major advantage of these models is that do not require fitted parameters for binary mixtures. Consequently, we will use a predictive approach to calculate the speed of sound. The speed of sound (*u*) given by SCFT [44] model is expressed in Eq. (7):

$$u = 1600\rho \left(\sum_{i=1}^{n_c} x_i s_i\right) \left(\sum_{i=1}^{n_c} x_i N_{av} m_i \frac{\pi}{6} d_i^3\right)$$
 (7)

where s_i represents the space filling factor of fluid i in the mixture, x_i denotes the liquid mole fraction, N_{av} is the Avogadro constant, and d_i is

the segment diameter dependent of temperature defined as PC-SAFT FoS.

On the other hand, NR model [45] proposes that speed of sound is given by Eq. (8):

$$u = \left(\frac{\sum_{i=1}^{n_c} \frac{x_i}{\rho_i} \mathbf{l} t^{1/3}}{\sum_{i=1}^{n_c} \frac{x_i}{\rho_i}}\right)^3$$
 (8)

with u_i , the experimental speed of sound for pure fluid.

In this study, the molar density present in both models (SCFT and NR) was obtained with PC-SAFT. For this reason, the approach to speed of sound modeling will also be called SCFT + PC-SAFT or NR + PC-SAFT.

2.3. Viscosity using FVT

Free volume theory (FVT) initially developed by Allan et al. [46–48] proposes that dynamic viscosity is defined as Eq. (9):

$$\eta = \eta^0 + \eta^{res} \tag{9}$$

The sum is composed of two terms, the first means viscosity for the dilute gas, while the second represents the residual viscosity.

The dilute gas viscosity is given by Chung et al. [55], but according to the literature [46–48,54], it is assumed that the term is negligible for liquids. Therefore, in this research we will use that FVT is given by Eq. (10):

$$\eta = \eta^{res} \tag{10}$$

Moreover, the residual viscosity given in mPa·s, is defined by Allan et al. [46-48] as Eq. (11):

$$\eta^{\text{res}} = 1000\widehat{\rho}l\left(\frac{\alpha + \frac{MP}{\widehat{\rho}}}{\sqrt{3MRT}}\right) exp\left[B\left(\frac{\alpha + \frac{MP}{\widehat{\rho}}}{2RT}\right)^{1.5}\right]$$
(11)

where R is the universal gas constant in $J \cdot \text{mol}^{-1} \cdot \text{K}^{-1}$, M is the molar mass in kg·mol⁻¹, P is the absolute pressure (in this study, experimental pressure was 10^5 Pa), $\widehat{\rho}$ represents the density in kg·m⁻³, which is obtained from PC-SAFT (in this work). This model has three fitted parameters with experimental viscosity data. These parameters are α , B, and l, which represents the barrier energy, free volume overlap, and characteristic molecular length. In order to obtain the residual viscosity in mPa·s, it's necessary that the previous fitted parameters be in the following units: $J \cdot \text{mol}^{-1}$, dimensionless, and m, respectively. It is important to note that Eq. (11) can be applied not only to pure fluids but also to mixtures, provided that the appropriate mixing rules are applied to the parameters (α , B, and l). In this study, the mixing rules were applied which assume the parameters vary quadratically with the mole fraction. Additionally, these mixing rules incorporate a total of three adjustable parameters. Therefore, these mixing rules are given by Eqs. (12–14):

$$\alpha = \sum_{i=1}^{2} \sum_{j=1}^{n_c} x_i x_j \sqrt{\alpha_i \alpha_j} (1 - l_{ij})$$
(12)

$$B = \sum_{i=1}^{2} \sum_{j=1}^{n_c} x_i x_j \sqrt{B_i B_j} (1 - w_{ij})$$
 (13)

$$l = \sum_{i=1}^{2} \sum_{j=1}^{n_c} x_i x_j \sqrt{l_i l_j} (1 - u_{ij})$$
 (14)

where l_{ij} , w_{ij} , and u_{ij} , are parameters that fit the experimental viscosity data for the binary mixtures. These fitted parameters are used to correct for interactions between i-j that affect the parameters (α , B, and l) for

the binary mixtures.

3. Results and discussion

3.1. Density

Density of ChCl/PA DES and its binary solutions with 1-butanol were measured in the temperature range (293.15 - 333.15) K and the experimental data is listed in Table 2. Fig. 1 displays the variation in density of binary solutions as a function of temperature. Experimental values are fitted to a second-degree polynomial equation in T (Eq. (15)).

$$\rho = a_{\rho} + b_{\rho}T + c_{\rho}T^2 \tag{15}$$

The fitting parameters $a_{\rho},\ b_{\rho},\ c_{\rho}$ and their standard deviation are summarized in Table S2.

Fig. 1 shows that density decreases linealy with increasing temperature for all compositions due to increased free volume resulting from added thermal energy. The second degree polynomial equation in T satisfacorily correlates the experimental data with temperature for all mole fractions as represented by correlation factor r^2 (Table S2, Supporting information).

Density which depends on molecular organization and packing and is influenced by vacancies present within the DES's liquid structure. Moreover, the composition changes and mole ratio of HBA and HBD in the DES are the means to modify the density of DES and its binary mixtures with 1-butanol.

At constant temperature ρ increases sharply with x_1 which gradually decreases with addition of more DES content in ChCl/PA + 1-butanol mixtures (Fig. S5, Supporting information). This non linear trend of ρ vs x_1 is fitted with 4th degree polynomial equation (Eq. S1, Supporting information) in x_1 (mole fraction of DES). The correlated parameters from experimental density data are listed in Table S3 (Supporting information).

Isobaric thermal expansion coefficient α_p is calculated using Eq. (16) [56]. The resulting values are tabulated in Table S4. Plots of α_p vs x_1 are shown in Fig. S6.

$$\alpha_p = \frac{1}{V} \left(\frac{\partial V}{\partial T} \right)_n = -\rho^{-1} \left(\frac{\partial \rho}{\partial T} \right)_n \tag{16}$$

 α_p is a property of fluids that uniquely describes volume expansion as a result of increase in temperature at constant pressure. Its knowledge is important for selecting a DES for a particular application. Its magnitude is found to decrease with increasing temperature at compositions, but at $x_1 \geq 0.7$ a reversal in trends is observed. This behaviour indicates a varying extent of hydrogen bond interactions between molecules of ChCl/PA DES compared to ChCl/PA DES and 1-butnaol in the mixtures. The increase in the magnitude of α_p indicated higher free volumes and wider spaces between the unbound molecules resulting in the decrease of density with respect to T [57].

The molar mass of ChCl/PA DES is calculated using Eq. (17) [58,59].

$$M_{ChCl/PADES} = M_{ChCl} x_{ChCl} + M_{PA} x_{PA}$$
 (17)

The lattice potential energy, U_{pot} represents energy required per mole to convert ionic solid into its gaseous components. In the case of DESs, it is dependent on the charge carried by its constituents and spaces between the ions.

The lattice potential energy U_{pot} and standard molar entropy, S^0 of pure ChCl/PA DES are calculated in the entire temperature range using empirical Eqs. (18) and (19), respectively [60].

$$U_{pot} = 1981.2 \left(\rho / M_{ChCl/PADES} \right)^{1/3} + 103.8 \tag{18}$$

$$S^0 = 1246.5V + 29.5 \tag{19}$$

where V is the molecular volume in nm³ ($V = 10^{21} * V_m/N_A$). The

Table 2 Density, $\rho/\text{kg.m}^{-3}$, of ChCl/PA and ChCl/PA DES + 1-butanol mixtures in the temperature range, $T=(293.15-333.15)\,\text{K}$ ($x_1=\text{mole fraction of ChCl/PA DES})$ and pressure, $p=0.1\,\text{MPa}$.

$x_1/T(K)$	$ ho/{ m kg.m^{-3}}$											
	293.15	298.15	303.15	308.15	313.15	318.15	323.15	328.15	333.15			
0.00	809.580	805.790	801.950	798.100	794.220	790.240	786.120	782.140	778.050			
0.10	854.237	852.284	849.681	847.670	845.659	844.006	842.101	840.304	838.323			
0.20	894.163	892.012	890.223	887.938	886.097	884.059	882.418	880.578	878.896			
0.30	928.415	926.266	924.359	922.544	920.750	918.845	916.899	914.913	912.888			
0.40	958.185	956.192	954.188	952.145	950.314	948.179	945.919	943.840	941.931			
0.50	980.277	978.069	975.904	974.058	972.324	970.688	968.951	967.388	965.651			
0.60	997.438	995.650	993.831	992.164	990.568	989.067	987.665	986.251	985.091			
0.70	1015.44	1013.48	1011.56	1009.88	1008.41	1007.07	1005.74	1004.54	1003.49			
0.80	1034.85	1032.02	1029.52	1027.23	1025.41	1023.51	1021.85	1020.63	1019.52			
0.90	1055.79	1051.86	1048.72	1045.49	1042.19	1039.02	1036.01	1032.80	1030.36			
1.00	1079.24	1074.81	1071.40	1068.02	1064.64	1061.27	1057.92	1054.58	1051.26			

Standard uncertainties, u, in T, x_1 , p and ρ are u (T) = 0.01 K, u (x_1) = 0.01, u(p) = 10kPa, and $u(\rho)$ = 0.003kg.m⁻³.

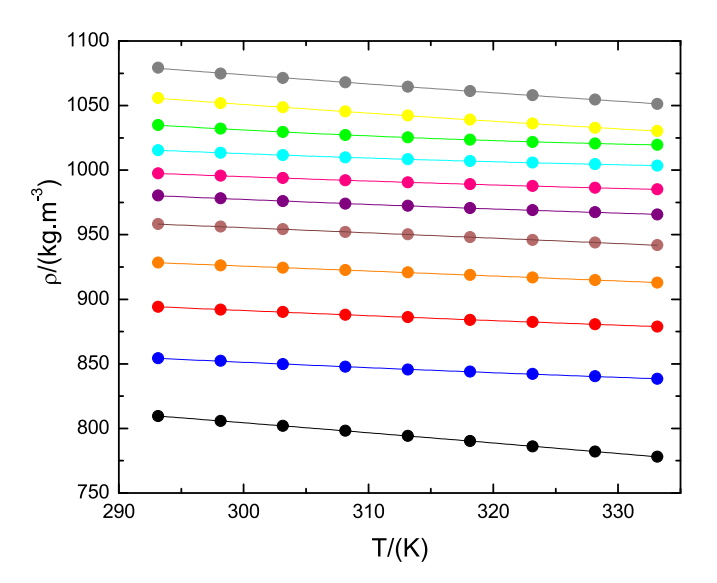


Fig. 1. Temperature dependence of density, ρ of ChCl/PA DES + 1-butanol mixtures for different mole fractions of ChCl/PA DES, $x_1 = (\bullet(\text{black}): 0.0; \bullet(\text{blue}): 0.1; \bullet(\text{red}): 0.2; \bullet(\text{orange}): 0.3; \bullet(\text{brown}): 0.4; \bullet(\text{purple}): 0.5; \bullet(\text{pink}): 0.6; \bullet(\text{cyan}): 0.7; \bullet(\text{green}): 0.8; \bullet(\text{yellow}): 0.9; \bullet(\text{gray}): 1.0).$ The solid lines are the best fit representation of Eq. (15). (For interpretation of the references to colour in this figure legend, the reader is referred to the web version of this article.)

calculated values of U_{pot} , S^0 and V in (293.15 – 333.15) K range are collected in Table S5 (Supporting information). U_{pot} values for ChCl/PA DES are lower compared to ionic crystal CsI ($U_{pot}=613kJ/mol$) which reflects its liquid state at room temperature [61]. The standard entropy, S^0 of ChCl/PA DES has increased slightly with increasing temperature. S^0 values for DES and ILs are relatively higher as compared to inorganic salts NaCl and KCl whose values are 72.1 and 82.6 kJ.K $^{-1}$ mol $^{-1}$ [62], indicating more disordered structures due to low electrostatic energy and reduced charge density [63,64].

To understand the non-ideal behavior, molecular interactions, and structural arrangements between ChCl/PA DES and cosolvent, excess molar volume V^E of ChCl/PA DES + 1-butanol binary mixtures were calculated from experimental density data (Table 1) according to Eq. (20).

$$V^{E} = \sum_{i=1}^{2} (x_{i} M_{i}) \left(\rho^{-1} - \rho_{i}^{-1} \right)$$
 (20)

where x_i , M_i and ρ_i represent mole fraction, molar mass, and density of component i respectively and ρ is density of binary mixtures.

The calculated V^E values are collected in Table 3 and plots of V^E vs x_1 (x_1 = mole fraction of ChCl/PA DES) are shown in Fig. 2.

Fig. 2 shows that values of V^E are negative for entire range of composition and temperature investigated. The positive or negative sign associated with the magnitude of the excess property $(V^E, \Delta \kappa_S, \Delta \eta)$ signifies the nature and presence of physical, chemical or structural type interaction forces between components of the solution, and their contributions to the excess property. The negative V^E values of the investigated system indicate presence of hydrogen bonding and attractive forces which could be ion-dipole, dipole-dipole, or charge transfer complex formation between DES and cosolvent molecules leading to volume contraction. The positive sign of V^E is indicative of weak physical interactions (van der Waals forces) among component of the mixture. The structural effect is either due to (1) interstitial fitting of a component molecule into other's structure producing a more compact geometric structure or (2) steric hinderance or unfavorable accomodation of component molecules [65]. The negative V^E signifies the predominance of hydrogen bonding between self associated components in solution. The magnitude of $|V^E|$ increases with increasing temperature. There are two effects operating at higher temperatures (a) thermal expansion of the system (b) breakage of the self associated structures of the cosolvent. The net effect appears in the increase of $|V^E|$ since now more free butanol molecules are available to interact with DES molecules (H-bonding). The effect is dominant at lower mole fractions below $x_1 = 0.5$. At higher mole fractions ($x_1 > 0.5$) increase in ChCl/PA DES molecules weakened hydrogen bond. Effect of increase in x_1 (i.e., ChCl/ PA DES molecules) is to lower $|V^E|$ at all mole fractions [59]. Generally, 1-butanol molecules form stronger self associated structures via hydrogen bonding compared to other isomers [66]. Recent studies have shown strong hydrogen bonding interaction in SDS/1-butanol and DBE/ 1-butanol mixtures [62,67].

Fig. 2 clearly represents the temperature and mole fraction dependence of V^E for ChCl/PA DES + 1-butanol system and its behavioral change at $x_1 \approx 0.35$ [68,69].

Redlich – Kister (R-K) equation is used to analyze the thermo – acoustic parameters which are defined as the difference between experimental values and ideal mixture values. Algebraic sign associated with the parameter is interpreted in terms of the intermolecular interactions present in liquid mixtures. The magnitude is a measure of the nonideality of the system due to associative or other interactions. Positive values indicate the presence of strong intermolecular interactions, and the negative values arise from the presence of weak interactions. R-K equation is thus an approach to analyze and discuss solute – solvent interactions and identify the nature of interactions.

The combined Redlich-Kister (CNIBSR-K) model at constant temperature explains the relationship between excess molar property $(V^E,$

Table 3 Excess molar volume, $10^6 \times V^E$, m^3 .mol⁻¹, of ChCl/PA DES + 1-butanol mixtures at different temperatures.

$x_1/T(K)$	$ extbf{\emph{V}}^{ extbf{\emph{E}}} imes 10^6/ extbf{m}^3. extbf{mol}^{-1}$											
	293.15	298.15	303.15	308.15	313.15	318.15	323.15	328.15	333.15			
0.00	0	0	0	0	0	0	0	0	0			
0.10	-1.967	-2.186	-2.337	-2.553	-2.776	-3.051	-3.317	-3.584	-3.847			
0.20	-3.249	-3.455	-3.688	-3.874	-4.111	-4.340	-4.625	-4.880	-5.166			
0.30	-3.871	-4.081	-4.295	-4.521	-4.753	-4.987	-5.230	-5.461	-5.701			
0.40	-4.028	-4.253	-4.449	-4.643	-4.862	-5.062	-5.263	-5.472	-5.708			
0.50	-3.485	-3.688	-3.857	-4.056	-4.270	-4.501	-4.733	-4.974	-5.209			
0.60	-2.524	-2.759	-2.945	-3.146	-3.357	-3.583	-3.827	-4.064	-4.331			
0.70	-1.660	-1.874	-2.038	-2.223	-2.430	-2.654	-2.884	-3.122	-3.380			
0.80	-0.936	-1.072	-1.173	-1.290	-1.450	-1.608	-1.790	-2.008	-2.240			
0.90	-0.359	-0.399	-0.433	-0.456	-0.474	-0.504	-0.548	-0.573	-0.667			
1.00	0	0	0	0	0	0	0	0	0			

Standard uncertainties, u in T, x_1 , p and ρ are u(T) = 0.01 K (for density), $u(x_1) = 0.01$, u(p) = 10kPa, $u(\rho) = 0.003$ kg.m $^{-3}$, $u(V^E) = 0.12 \times 10^{-6}$ m 3 .mol $^{-1}$.

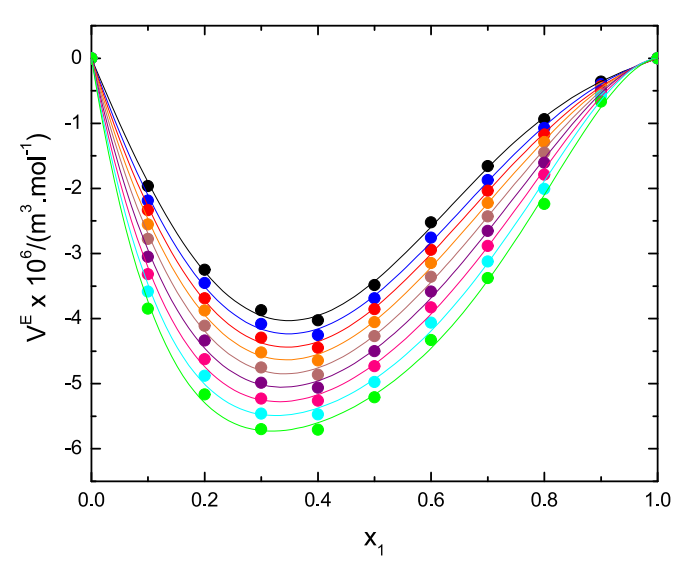


Fig. 2. Variation of excess molar volume, $V^E \times 10^6 \text{m}^3 \cdot \text{mol}^{-1}$ of ChCl/PA DES + 1-butanol mixtures with mole fraction of ChCl/PA DES, x_1 in the temperature range 293.15 ≤ T/K ≤ 333.15 (\bullet (black): 293.15 K; \bullet (blue): 298.15 K; \bullet (red): 303.15 K; \bullet (orange): 308.15; \bullet (brown): 313.15 K; \bullet (purple): 318.15 K; \bullet (pink): 323.15 K; \bullet (cyan): 328.15 K; \bullet (green): 333.15 K). The solid lines connecting the data points are the best fit representation of Eq. (21).

 $\Delta \kappa_S$, $\Delta \eta$) and composition as given by Eq. (21) [68,70–72].

$$Y^{E} = x_{ChCl/PADES} x_{1-Butanol} \sum_{i=0}^{k} A_{j} (x_{ChCl/PADES} - x_{1-Butanol})^{j}$$
(21)

where, $Y^E = (V^E, \Delta \kappa_S \ and \ \Delta \eta)$, $x_{ChCl/PADES} =$ mole fraction of ChCl/PA DES (component 1), $x_{1-Butanol} =$ mole fraction of 1-butanol (component 2), $A_j =$ Adjustable binary coefficients, j = degree of polynomial equation.

Parametric fitting of the excess property Y^E by least square method provides useful information which helps to understand interactions between components of a binary mixture. The numerical values of j can be varied to find an accurate mathematical representation of experimental data.

The calculated V^E values are satisfactorily fitted to a third order Redlich-Kister polynomial (Eq. (21)) as shown by the solid lines in Fig. 2 and the results of adjustable polynomial coefficients (A_j 's) and their standard deviations (σ) are summarized in Table S6 (Supporting information).

Further understanding of solute-solvent and solute-solute in-

teractions in binary mixtures of ChCl/PA DES and 1-butanol is obtained by calculating the apparent molar volume $(V_{\emptyset,i})$, partial molar volume $(\overline{V_i})$, and excess partial molar volume $(\overline{V_i})$ of individual components using Eqs. (22–24), respectively.

$$V_{\phi,i} = V_{m,i} + \frac{V^E}{x_i} \tag{22}$$

$$\overline{V_i} = V_{m,i} + V^E + (1 - x) \left(\frac{\partial V^E}{\partial x_i} \right)_{PT}$$
(23)

$$\overline{V}_{i}^{E} = \overline{V}_{i} - V_{m,i} \tag{24}$$

 $V_{m,i}$ is the molar volume of the pure component i. The calculated values of $V_{\emptyset,i}$, $\overline{V_i}$ and $\overline{V_i^E}$ of individual components [(i=1 (ChCl/PA DES), i=2 (1-butanol)] are collected in Tables S7–S12 (Supporting information).

The calculated $V_{\phi,i}$ values are positive for both ChCl/PA DES and 1-butanol, indicating strong interaction and favorable structural effects between DES and 1-butanol molecules [73]. The calculation of partial molar volume of individual components at infinite dilution $(\overline{V}_i^{\infty})$ are of interest because the solute–solute interactions are negligible and only solute – solvent interactions become important. Values of \overline{V}_1^{∞} for ChCl/PA DES and \overline{V}_2^{∞} for 1-butanol are calculated in the entire temperature range (293.15 –333.15)K using Eqs. (25) and (26) respectively and collected in Table S13.

$$\overline{V}_{1}^{\infty} = V_{m,1} + \sum_{i=1}^{n} A_{i} (-1)^{i}$$
(25)

$$\overline{V}_2^{\infty} = V_{m,2} + \sum_{i=1}^n A_i \tag{26}$$

Plots of \overline{V}_i^{∞} vs x_1 are shown in Fig. S6 (Supporting information).

3.2. Speed of sound

The speed of sound, u and the derived parameter isentropic compressibility κ_s provide useful information on intermolecular interactions between components in fluid phase. Many properties such as the isothermal expansion coefficient, the Joule-Thomson coefficient and isochoric heat capacity which depend on density and speed of sound are important in the designing of a process [74]. The experimental data for speed of sound u of ChCl/PA DES, 1-butanol and their binary mixtures is tabulated in Table 4 and u as function of T is plotted for entire range of composition in Fig. 3.

Fig. 3 shows that the u decreases with increasing T and this behavior is consistent for the entire range of composition at

Table 4 Speed of sound, $u/m.s^{-1}$ of ChCl/PA DES + 1-butanol mixtures as a function of temperature, T = (293.15 - 333.15) K and pressure, p = 0.1MPa.

$x_1/T(K)$	$u/\mathrm{m.s^{-1}}$	$u/m.s^{-1}$											
	293.15	298.15	303.15	308.15	313.15	318.15	323.15	328.15	333.15				
0.00	1256.3	1239.3	1222.4	1205.5	1188.8	1173.0	1156.5	1140.1	1123.6				
0.10	1289.3	1271.9	1254.6	1237.5	1220.3	1203.1	1186.1	1169.1	1152.1				
0.20	1328.3	1311.3	1294.3	1277.5	1261.2	1244.5	1227.8	1210.9	1194.1				
0.30	1390.3	1373.9	1357.4	1341.1	1324.7	1308.3	1292.0	1275.6	1259.2				
0.40	1459.7	1443.5	1427.3	1411.2	1395.1	1379.0	1362.9	1346.8	1330.3				
0.50	1507.6	1491.6	1475.8	1459.9	1444.2	1428.5	1412.8	1397.0	1381.3				
0.60	1566.2	1550.6	1535.0	1519.4	1504.0	1488.5	1473.1	1457.6	1442.2				
0.70	1631.0	1615.6	1600.5	1585.5	1570.5	1555.5	1540.5	1525.6	1510.7				
0.80	1728.3	1714.2	1700.1	1685.9	1671.6	1657.4	1643.2	1629.0	1614.8				
0.90	1830.6	1816.7	1802.8	1789.1	1775.4	1761.7	1748.2	1734.8	1721.5				
1.00	1945.3	1934.7	1925.8	1918.3	1911.8	1904.6	1895.5	1887.3	1876.4				

Standard uncertainties, u, in T, x, P and u are u(T) = 0.01 K, $u(x_1) = 0.01$, u(p) = 10kPa and u(u) = 0.5m.s $^{-1}$.

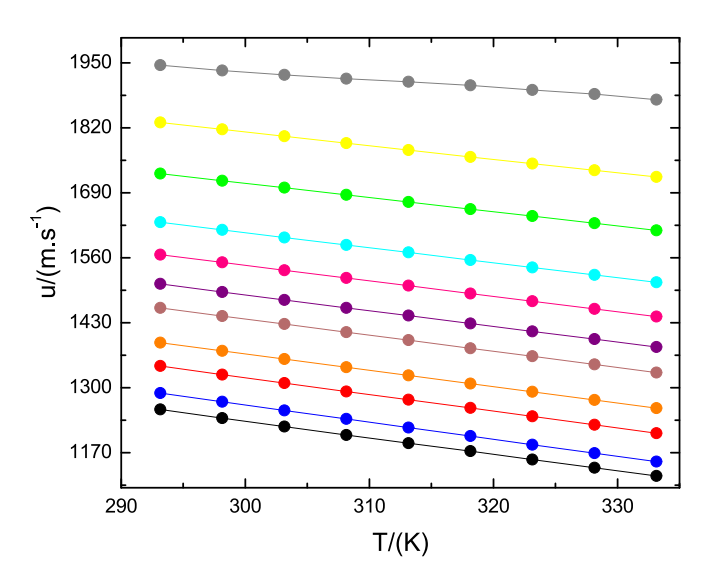


Fig. 3. Temperature dependence of speed of sound, u of the binary mixture, ChCl/PA DES + 1 butanol with varying $x_1 = (\bullet(\text{black}): 0.0; \bullet(\text{blue}): 0.1; \bullet(\text{red}): 0.2; \bullet(\text{orange}): 0.3; \bullet(\text{brown}): 0.4; \bullet(\text{purple}): 0.5; \bullet(\text{pink}): 0.6; \bullet(\text{cyan}): 0.7; \bullet(\text{green}): 0.8; \bullet(\text{yellow}): 0.9; \bullet(\text{gray}): 1.0).$ The solid lines connect the experimental data points.

 $T=(293.15-333.15){\rm K}$ range. There is slowing down of sound waves due to increased spaces in component molecules in less dense medium. However, with increasing DES content in binary mixture, the value of u increases as the medium of sound waves becomes denser.

The acoustic property, isentropic compressibility κ_S is defined in terms of fluid density (ρ) and speed of sound (u) by Newton's Laplace Eq. (27).

$$\kappa_S = -V^{-1} \left(\frac{\partial V}{\partial P} \right)_S = u^{-2} \rho^{-1} \tag{27}$$

The validity of Eq. (23) depends on the fact that the perturbation to the liquid sample produced by the acoustic wave does not relax completely during the time constant of that wave [75]. κ_S measures the relative change in the volume of fluid with corresponding change in pressure. The κ_S values (Table 5) decrease as ChCl/PA DES content of the solution is increased in the temperature range studied which suggests tightening of the ChCl/PA DES and 1-butanol structure in binary mixtures [76].

The effect of increasing temperature on κ_S is just the opposite of that observed for increase in mole fraction of ChCl/PA DES. The temperature dependence of κ_S is explained in Fig. 4.

Isentropic compressibility deviation, $\Delta\kappa_S$ represents the changes effected in the solvent by solute molecules because of solute – solvent interactions in binary mixtures when the concentration of the latter approaches zero [73]. κ_S for ChCl/PA DES + 1-butanol system is calculated by following Eq. (28) and tabulated in Table 6.

$$\Delta \kappa_S = \kappa_S - \sum_{i=1}^2 x_i \kappa_{s,i} \tag{28}$$

where x_i and $\kappa_{s,i}$ are mole fractions and isentropic compressibility of

Table 5 Isentropic compressibility, $\kappa_S \times 10^{12}/\text{Pa}^{-1}$ of ChCl/PA DES + 1-butanol mixtures as a function of temperature, T.

$x_1/T(K)$	$\kappa_{S} \times 10^{12}/\text{Pa}$	1-1							
	293.15	298.15	303.15	308.15	313.15	318.15	323.15	328.15	333.15
0.00	782.6	808.0	834.6	862.1	890.9	919.7	951.1	983.7	1018.1
0.10	704.2	725.2	747.7	770.4	794.1	818.5	844.1	870.7	898.7
0.20	619.8	637.3	655.2	674.2	693.0	713.1	733.7	755.6	778.3
0.30	557.2	572.0	587.1	602.7	618.9	635.9	653.4	671.8	690.9
0.40	489.8	501.9	514.5	527.4	540.6	554.6	569.2	584.1	599.9
0.50	448.9	459.5	470.5	481.7	493.1	504.9	517.1	529.7	542.7
0.60	408.7	417.7	427.0	436.6	446.3	456.3	466.6	477.2	488.1
0.70	370.2	378.0	385.9	393.9	402.1	410.4	419.0	427.7	436.6
0.80	323.5	329.7	336.1	342.5	349.0	355.7	362.5	369.2	376.2
0.90	282.6	288.1	293.4	298.8	304.4	310.1	315.8	321.7	327.5
1.00	244.9	248.6	251.7	254.4	257.0	259.7	263.1	266.2	270.2

Standard uncertainties, u, in T, x, P and u are u(T)=0.01 K, u (x_1) = 0.01, u(p)=10kPa and u(u)=0.5m.s $^{-1}$.

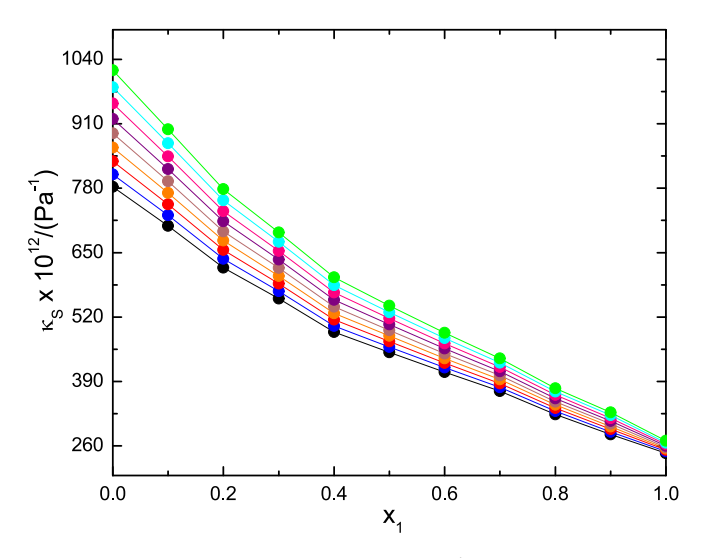


Fig. 4. Isentropic compressibility, $\kappa_S \times 10^{12}/\text{Pa}^{-1}$, of ChCl/PA DES + 1 butanol mixtures as a function of x_1 , in the temperature range 293.15 \leq T/K \leq 333.15 \bullet (black): 293.15 K; \bullet (blue): 298.15 K; \bullet (red): 303.15 K; \bullet (orange): 308.15; \bullet (brown): 313.15 K; \bullet (purple): 318.15 K; \bullet (pink): 323.15 K; \bullet (cyan): 328.15 K; \bullet (green): 333.15 K). The solid lines connect the values are calculated from Eq. (27).

component i, respectively.

Functional dependence of $\Delta \kappa_S$ on x_1 (Fig. 5) is similar to that observed in the case of V^E , emphasizing identical nature of contributing factors to inter molecular interaction.

The $\Delta\kappa_S$ values are negative over the entire range of composition and temperature (293.15 –333.15)K but the magnitude is larger compared to V^E indicating that sound waves have greatly disturbed the system enforcing stronger interactions between unlike molecules of ChCl/PA DES and 1-butanol. The specific (dipole–dipole) interaction favors the better geometric fitting of component molecules of unequal size into one another.

The experimental values for $\Delta \kappa_S$ are fitted to Redlich Kister polynomial Eq. (21) and correlated parameters are tabulated in Table S14 (Supporting information).

Intermolecular free length, L_f (Eq. (29)) expresses the compressibility behavior of DES under the influence of temperature, molecular mass, and mole ratio of DES with cosolvent.

$$L_f = K \sqrt{\frac{1}{\rho u^2}} \tag{29}$$

where K is Jacobson's constant, a temperature dependent parameter

[77]. The calculated values of L_f are presented in Table 7 and the plot of L_f vs x_1 at T=(293.15-333.15) K is shown in Fig. 6.

The influence of increasing temperature and DES content in solution on L_f values are in opposition. The slowing down of speed of sound at higher temperatures allows larger space between molecules. On the other hand, L_f values decreased with increasing concentration of DES reflects reduced free space indicating compactness of the structure [63].

Acoustic impedance Z, which measures the resistance experienced by the passage of ultrasound beam through the medium [78], is calculated using Eq. (30).

$$Z = \rho.u \tag{30}$$

The calculated values of Z (Eq. (30)) are presented in Table 8 and plotted vs x_1 in Fig. 7.

Increase in the Z values with increasing temperature indicates somewhat loosening of the structure that leads to increase in available free space for the passage of sound waves. With increasing concentration of ChCl/PA DES, decrease in Z value is expected, as compaction of the system takes place due to increase in charge centers. These two trends are complemented by temperature and concentration dependence of L_f .

Variation in these properties ($\Delta \kappa_S$, L_f and Z) offer qualitative description of behavior of binary mixture (ChCl/PA DES + 1-butanol) in intermediate composition range [79].

3.3. Viscosity

Viscosity η is an important physical property which explain the internal resistance to fluid for shear stress. For many chemical engineering applications, viscosity data at different temperatures is required to optimize process designing. The viscosity of DES can be manipulated by addition of suitable cosolvents for mass transfer rates in solutions [80]. Experimentally measured η of ChCl/PA DES and its binary mixtures with 1-butanol in the temperature range $293.15 \le T/K \le 333.15$ is recorded in Table 9.

The viscosity decreases with increasing mole fraction of ChCl/PA DES in binary mixtures (Fig. S8, Supporting information). This is due to the weakening of intermolecular forces among the components of mixtures [56]. The fourth-degree polynomial equation correlates the experimentally measured viscosity with T for all mole fractions (x_1 = mole fraction of ChCl/PA DES) and the correlated parameters are reported in Table S15 (Supporting information).

The experimental transport property, dynamic viscosity (η)is satisfactorily correlated with temperature T by Vogel-Fulcher-Tammann (VFT) Eq. (31).

$$\ln\left(\frac{Y}{Y^0}\right) = \ln\left(\frac{A_Y}{Y^0}\right) + \frac{B_Y}{\left(T - T_{0,Y}\right)} \tag{31}$$

Table 6 Isentropic compressibility deviation, $\Delta\kappa_S \times 10^{12}/Pa^{-1}$ of ChCl/PA DES + 1 butanol mixtures at different temperature T.

$x_1/T(K)$	$\Delta \kappa_{\rm S} imes 10^{12}/{ m Pa}^{-1}$											
	293.15	298.15	303.15	308.15	313.15	318.15	323.15	328.15	333.15			
0.00	0	0	0	0	0	0	0	0	0			
0.10	-24.59	-26.85	-28.59	-31.02	-33.41	-35.15	-38.19	-41.20	-44.59			
0.20	-55.27	-58.80	-62.74	-66.41	-71.17	-74.62	-79.73	-84.56	-90.18			
0.30	-64.05	-68.23	-72.56	-77.11	-81.79	-85.84	-91.31	-96.67	-102.8			
0.40	-77.71	-82.32	-86.95	-91.66	-96.69	-101.1	-106.7	-112.5	-119.0			
0.50	-64.87	-68.76	-72.60	-76.61	-80.82	-84.83	-90.02	-95.29	-101.4			
0.60	-51.23	-54.64	-57.79	-60.95	-64.24	-67.39	-71.71	-75.98	-81.28			
0.70	-35.98	-38.39	-40.61	-42.82	-45.11	-47.33	-50.51	-53.77	-57.91			
0.80	-28.92	-30.72	-32.17	-33.48	-34.75	-36.08	-38.24	-40.50	-43.57			
0.90	-16.00	-16.45	-16.56	-16.37	-15.98	-15.65	-16.07	-16.24	-17.46			
1.00	0	0	0	0	0	0	0	0	0			

Standard uncertainties, u, in T, x, P and u are u(T) = 0.01 K, $u(x_1) = 0.01$, u(p) = 10kPa and u(u) = 0.5m.s $^{-1}$, $u(\Delta \kappa_S) = 0.05 \times 10^{-12} Pa^{-1}$.

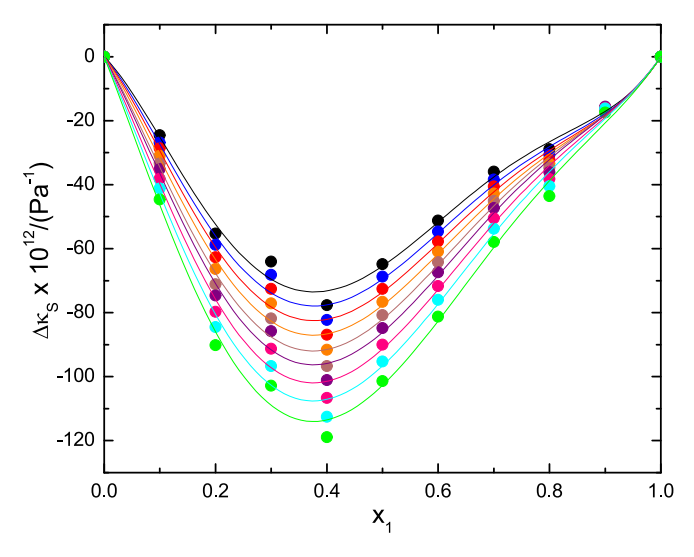


Fig. 5. Isentropic compressibility deviation, $\Delta\kappa_S \times 10^{12}/Pa^{-1}$, of ChCl/PA DES -1 butanol mixtures as a function of x_1 , in the temperature range $293.15 \le T/K \le 333.15$ (black): 293.15 K; (blue): 298.15 K; (red): 303.15 K; (orange): 308.15; (brown): 313.15 K; (purple): 318.15 K; (pink): 323.15 K; (cyan): 328.15 K; (green): 333.15 K). The solid lines are the best fit representation of Eq. (21).

where Y is viscosity η ($Y^0 = \eta^0 = 1mPa^{-1}$) and A_Y , B_Y and $T_{0,Y}$ are three adjustable parameters. Equation (31) fits the experimental data well for glass forming liquids as the system dynamics slows down on reaching the critical temperature $T_{0,Y}$ (also known as Vogel temperature). The $T_{0,Y}$ is typically 10-15 K less than the glass transition temperature, T_g of the system. VFT equation predicts the viscosity values in low temperature region due to divergence of viscosity at finite temperature [81,82]. A_Y represents the property Y (η) when T $\longrightarrow \infty$, and the quantity $E_a = B_Y \times R$ (where R is general gas constant) is the pseudo activation energy.

The functional dependance of η on T Eq. (31) is shown in Fig. 8. The three fitting parameters are tabulated in Table S15 (Supporting information).

Arrhenius Eq. (32) provides another model to explain temperature dependence of transport property (η) that has single adjustable parameter [83].

$$lnA = lnA_{\infty} + \frac{E_A}{RT}$$
 (32)

where A represents η , A_{∞} is an empirical constant, E_A is activation energy associated with the property A, R and T have their usual meaning. Arrhenius model is commonly used to investigate temperature dependence.

dent behavior of viscosity through plot of $\ln \eta$ against 1/T as shown in Fig. 9 and the corresponding fitting parameters of Eq. (32) are collected in Table S16 (Supporting information).

The mathematical formulation of Arrhenius equation points towards the monotonic increase of rate process with temperature. Fig. 9 shows that the plot of $\ln \eta$ vs T^{-1} is not perfectly linear. The Arrhenius equation is applicable in the limited temperature range (T < 2Tg). Temperature dependence of viscosity modeled by Arrhenius and VFT equations is also influenced by composition [84]. Hydrogen bonding and dipole–dipole interactions between like and unlike molecules at different mole fractions of ChCl/PA DES also become important in determining transport properties of fluids. Therefore, VFT equation provides a better fit of viscosity data due to its applicability in wide temperature range.

The viscosity deviation, $\Delta \eta$ is the difference between the experimentally measured viscosity of binary mixture and the average summation of viscosities of constituents' components (ChCl/PA DES and 1-butanol). The $\Delta \eta$ for binary mixtures is calculated using Eq. (33).

$$\Delta \eta = \eta - \sum_{i=1}^{2} x_i \eta_i \tag{33}$$

where x_i and η_i are mole fractions and dynamic viscosity of component i respectively. Calculated values of $\Delta \eta$ are collected in Table 10 and its plot as a function of x_1 is shown in Fig. 10 for all temperatures investigated.

Fig. 10 shows that $\Delta \eta$ values are negative over the entire range of composition and temperature, T = (293.15 - 333.15) K. The minimum in the $\Delta \eta$ vs T curves lie at $x_1 \approx 0.65$ which is deeper at lower temperature than the next higher temperature. In contrast, the volumetric (V^E) and accoustic $(\Delta \kappa_S)$ properties of the system show opposite trend for temperature variation i.e., minimum which lies in the vicinity of $x_1 \approx 0.35$ is deeper at higher temperature than at lower temperature. Similar behavior is also reported for binary solutions of [ChCl]:[Lev] (1:2) and ethanol, 1-propanol, 1-butanol and 1-pentanol studied at three temperatures [85]. Interpretation of the negative $\Delta \eta$ values in the light of V^E and $\Delta \kappa_S$ result suggests that the resistive forces in the solution are strongest in the vicinity of $x_1 \approx 0.65$ in the ChCl/PA DES region at lower temperatures. Resistive forces decrease on both ends of the minimum and as the temperature increases. The origin of the resistive forces could be attributed to the existence of hydrogen bonded structures between the components and between the molecules of cosolvent and their unlike shapes and sizes. The non ideal behavior as depicted by negative values of excess properties, is a complex function of molecular interactions in liquid phase, interstitial accommodation of smaller molecules and the size and shapes of molecules [86]. The calculated values of $\Delta \eta$ are fitted to Redlich Kister polynomial Eq. (21) and resulting correlated parameters are presented in Table S17 (Supporting information).

To model the properties (density, speed of sound, and dynamic vis-

Table 7 Intermolecular free length, $L_f \times 10^{11}/\text{m}$ of ChCl/PA DES + 1-butanol mixtures as a function of mole fraction, x_1 .

$x_1/T(K)$	$L_{f} imes10^{11}/ ext{m}$											
	293.15	298.15	303.15	308.15	313.15	318.15	323.15	328.15	333.15			
0.00	5.504	5.641	5.783	5.929	6.078	6.228	6.386	6.549	6.718			
0.10	5.221	5.345	5.474	5.604	5.738	5.875	6.017	6.162	6.312			
0.20	4.898	5.010	5.124	5.243	5.361	5.484	5.610	5.740	5.874			
0.30	4.644	4.746	4.851	4.957	5.066	5.178	5.293	5.412	5.534			
0.40	4.354	4.446	4.541	4.637	4.735	4.836	4.941	5.047	5.157			
0.50	4.168	4.254	4.342	4.431	4.522	4.614	4.709	4.806	4.905			
0.60	3.977	4.056	4.137	4.219	4.302	4.387	4.473	4.562	4.651			
0.70	3.785	3.859	3.933	4.007	4.083	4.160	4.239	4.318	4.399			
0.80	3.538	3.604	3.670	3.737	3.804	3.873	3.943	4.012	4.083			
0.90	3.308	3.368	3.429	3.490	3.553	3.616	3.680	3.745	3.810			
1.00	3.079	3.129	3.176	3.221	3.264	3.310	3.359	3.407	3.461			

Standard uncertainties, u, in T, x, P and u are u(T)=0.01 K, $u(x_1)=0.01$, u(p)=10kPa and u(u)=0.5m.s $^{-1}$.

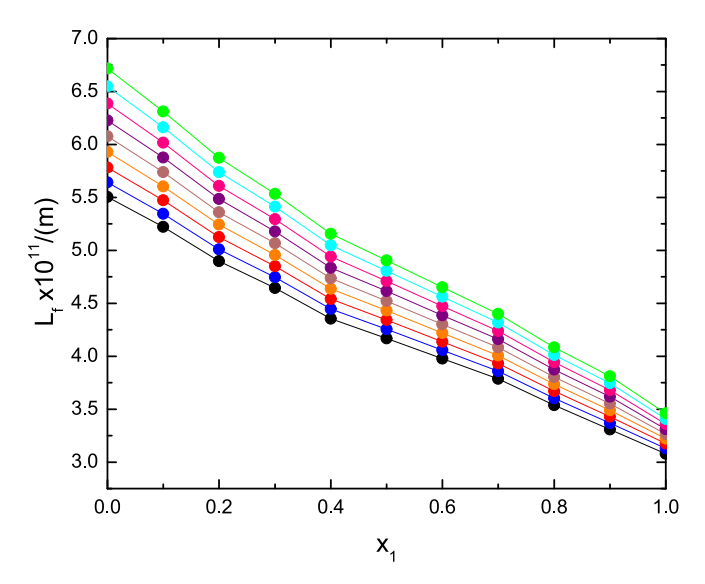


Fig. 6. Intermolecular free length, $L_f \times 10^{11}/\text{m}$, of ChCl/PA DES + 1 butanol mixtures as a function of x_1 , in the temperature range 293.15 \leq T/K \leq 333.15 \bullet (black): 293.15 K; \bullet (blue): 298.15 K; \bullet (red): 303.15 K; \bullet (orange): 308.15; \bullet (brown): 313.15 K; \bullet (purple): 318.15 K; \bullet (pink): 323.15 K; \bullet (cyan): 328.15 K; \bullet (green): 333.15 K). The solid lines represent the data are calculated from Eq. (29).

cosity) in the binary mixture composed by ChCl/PA DES + 1-butanol, the PC-SAFT EoS parameters for the pure fluids is necessary. For 1butanol, the optimal parameters using 2B scheme were obtained from the literature [87]. It is important to mention that literature studies establish two strategies for DES modeling, the first strategy consists of modeling using the pure fluid assumption [88], while the second consists of treating DES as a binary mixture [89,90]. The first approach would allow treating the DES + another component mixture as a binary mixture and would reduce the number of fitted parameters, while the second approach considers DES as a binary mixture and the DES \pm another component mixture as a ternary mixture; this considers a greater number of fitted parameters due to the presence of each binary that forms it than the ternary mixture. For the case of DES (a binary mixture of ChCl/PA in a 1:2 M ratio), this research assumes that it behaves as a pure fluid, i.e., treating it as a pseudo pure fluid as 2B scheme (one positive site in PA which is HBD and one negative site in ChCl which is HBA). This assumption (DES as pseudo pure fluid) is supported by the literature for several reasons [51-53,91]: to avoid ternary mixture, to prevent an increase in fitted parameters (five parameters for ChCl pure fluid parameters and five parameters for PA pure fluid), and to avoid additional fitted parameters for the three binary mixtures forming the ternary system; If the binary interaction parameter were temperature-dependent, six fitted parameters in total would be required, compared to only two used in this study. The results discussed in the cited literature reveal a strong consistency between theoretical and experimental data for pseudo binary mixtures that include DES and the other substance. Therefore, in this manuscript we use the experimental liquid density data for the DES along with the objective function given by Eq. (34):

$$OF\left(m, \sigma, \frac{\varepsilon}{k_B}, \frac{\varepsilon^{AB}}{k_B}, \kappa^{AB}\right) = \min \sum_{i=1}^{N} \left(\frac{\rho_i^{exp.} - \rho_i^{theo.}}{\rho_i^{exp.}}\right)^2$$
(34)

where, *theo.* and *exp.* are related to the calculated value with the theoretical model and experimental value, respectively. Moreover, N represents the number of experimental data. The fitted parameters for DES were obtained in the temperature range of (293.15 K - 333.15) K. The parameters for 1-butanol and DES are summarized in Table 11:

The average absolute deviations in density for 1-butanol and DES were 0.11~% and 0.06~%, respectively. The values are calculated using the Eq. (35):

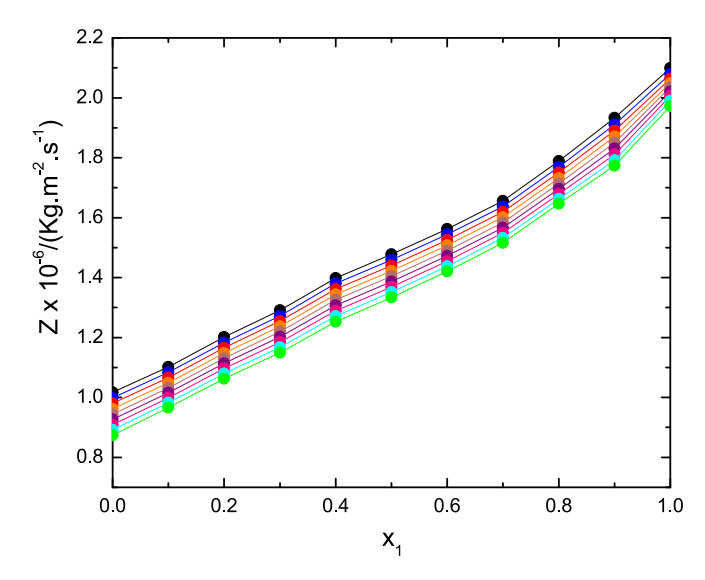


Fig. 7. Acoustic impedance, $Z \times 10^{-6}$ /kg.m $^{-2}$.s $^{-1}$, of ChCl/PA DES + 1 butanol mixtures as a function of x_1 , in the temperature range 293.15 ≤ T/K ≤ 333.15 •(black): 293.15 K; •(blue): 298.15 K; •(red): 303.15 K; •(orange): 308.15; •(brown): 313.15 K; •(purple): 318.15 K; •(pink): 323.15 K; •(cyan): 328.15 K; •(green): 333.15 K). The solid lines connect the data points are calculated from Eq. (30).

Table 8 Acoustic impedance, $Z \times 10^{-6} / \text{kg.m}^{-2} \cdot \text{s}^{-1}$ of ChCl/PA DES + 1-butanol mixtures as a function of mole fraction, x_1

$x_1/T(K)$	$ extbf{Z} imes 10^{-6}/ ext{kg}$	$Z \times 10^{-6}$ /kg.m ⁻² .s ⁻¹											
	293.15	298.15	303.15	308.15	313.15	318.15	323.15	328.15	333.15				
0.00	1.017	0.999	0.980	0.962	0.944	0.927	0.909	0.892	0.874				
0.10	1.101	1.084	1.066	1.049	1.032	1.015	0.999	0.982	0.966				
0.20	1.201	1.183	1.166	1.148	1.131	1.113	1.097	1.080	1.063				
0.30	1.291	1.273	1.255	1.237	1.220	1.202	1.185	1.167	1.150				
0.40	1.399	1.380	1.362	1.344	1.326	1.308	1.289	1.271	1.253				
0.50	1.478	1.459	1.440	1.422	1.404	1.387	1.369	1.351	1.334				
0.60	1.562	1.544	1.526	1.508	1.490	1.472	1.455	1.438	1.421				
0.70	1.656	1.637	1.619	1.601	1.584	1.566	1.549	1.533	1.516				
0.80	1.789	1.769	1.750	1.732	1.714	1.696	1.679	1.663	1.646				
0.90	1.933	1.911	1.891	1.870	1.850	1.830	1.811	1.792	1.774				
1.00	2.099	2.079	2.063	2.049	2.035	2.021	2.005	1.990	1.973				

Standard uncertainties, u, in T, x, P and u are u(T) = 0.01 K, $u(x_1) = 0.01$, u(p) = 10kPa and u(u) = 0.5m.s⁻¹.

Table 9 Dynamic viscosity, η /mPa.s of ChCl/PA DES + 1 butanol mixtures as a function of temperature T = (293.15 - 333.15) K and pressure, p = 0.1MPa.

$x_1/T(K)$	η/m Pa.s											
	293.15	298.15	303.15	308.15	313.15	318.15	323.15	328.15	333.15			
0.00	2.954	2.608	2.251	1.987	1.731	1.553	1.420	1.315	1.257			
0.10	3.541	3.058	2.657	2.330	2.049	1.815	1.619	1.451	1.366			
0.20	3.591	3.112	2.746	2.443	2.163	1.889	1.709	1.545	1.459			
0.30	3.881	3.349	2.908	2.543	2.229	1.985	1.769	1.597	1.512			
0.40	4.246	3.719	3.284	2.923	2.542	2.216	2.000	1.811	1.652			
0.50	4.769	4.224	3.796	3.313	2.900	2.555	2.266	2.016	1.818			
0.60	10.90	9.461	8.001	6.669	5.921	5.288	4.737	4.297	3.977			
0.70	16.33	13.71	11.61	9.946	8.582	7.454	6.545	5.795	5.221			
0.80	32.78	26.80	22.17	18.80	16.12	13.76	11.73	10.08	8.793			
0.90	38.35	31.09	25.57	21.34	18.18	15.67	13.35	11.43	9.831			
1.00	57.26	46.66	37.75	31.04	25.86	21.77	18.67	16.25	14.03			

Standard uncertainties, u, in T, x, P and η are u(T)=0.02 (for viscosity) K, $u(x_1)=0.01$, u(P)=10kPa and $u(\eta)=0.01$ mPa.S.

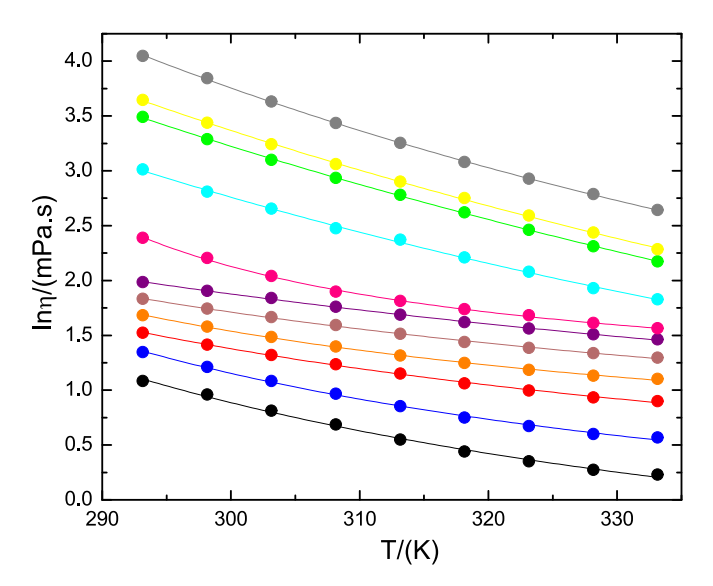


Fig. 8. Temperature and composition dependence of dynamic viscosity η for pure ChCl/PA DES, 1-butanol and their binary mixtures measured at atmospheric pressure, $x_1 = (\bullet(\text{black}); 0.0; \bullet(\text{blue}); 0.1; \bullet(\text{red}); 0.2; \bullet(\text{orange}); 0.3; \bullet(\text{brown}); 0.4; \bullet(\text{purple}); 0.5; \bullet(\text{pink}); 0.6; \bullet(\text{cyan}); 0.7; \bullet(\text{green}); 0.8; \bullet(\text{yellow}); 0.9; \bullet(\text{gray}); 1.0). The solid lines are the best fit representation of Eq. (31).$

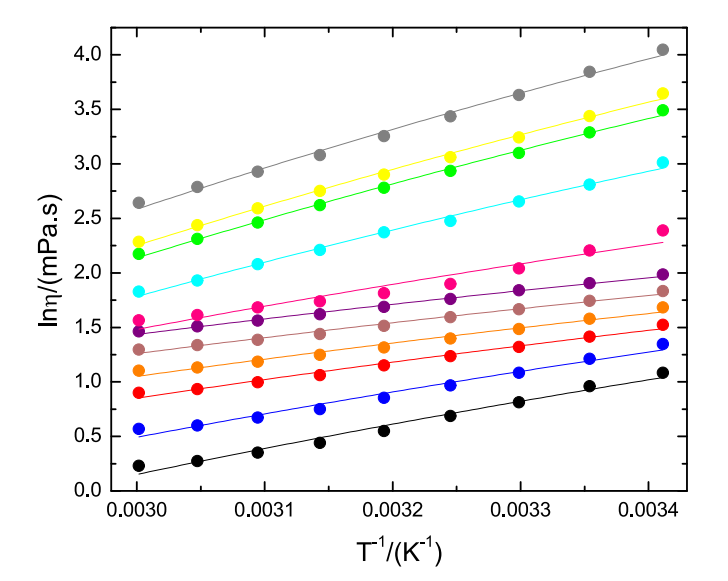


Fig. 9. Temperature and composition dependence of viscosity for pure ChCl/PA DES, 1-butanol and their binary mixtures measured at atmospheric pressure, $x_1 = (\bullet(\text{black}): 0.0; \bullet(\text{blue}): 0.1; \bullet(\text{red}): 0.2; \bullet(\text{orange}): 0.3; \bullet(\text{brown}): 0.4; \bullet(\text{purple}): 0.5; \bullet(\text{pink}): 0.6; \bullet(\text{cyan}): 0.7; \bullet(\text{green}): 0.8; \bullet(\text{yellow}): 0.9; \bullet(\text{gray}): 1.0). The solid lines are the best fit representation of Eq. (32).$

$$AAD\Psi (\%) = \frac{100}{N} \sum_{i=1}^{N} \frac{\left| \Psi_{i}^{exp.} - \Psi_{i}^{theo.} \right|}{\Psi_{i}^{exp.}}$$
(35)

where, Ψ is the property (density, speed of sound, and viscosity). Therefore, our model correctly estimates the experimental DES and 1-butanol density data. To model the experimental density data of the DES + 1-butanol mixture, a linear correlation for the binary interaction parameter is applied, i.e., the binary interaction parameter is fitted to the experimental data using the linear form $(k_{ij} = a_{ij} + b_{ij} \bullet T)$. Consequently, k_{ij}^T is fitted for each temperature using Eq. (36), while the parameters a_{ij} and b_{ij} are optimized using Eq. (37) and at nine experimental temperatures.

$$OF(k_{ij}^{T}) = \min \sum_{i=1}^{N} \left(\frac{\rho_i^{exp.} - \rho_i^{theo.}}{\rho_i^{exp.}} \right)^2$$
(36)

$$OF(a_{ij}, b_{ij}) = \min \sum_{i=1}^{9} \left(\frac{k_{ij}^T - k_{ij}}{k_{ij}^T}\right)^2$$
 (37)

Therefore, we have obtained $k_{ij} = 0.695017 - 0.00287885 \bullet T/K$ and the AAD (%) of 0.41 %. The binary interaction parameter decreases with temperature and negative values at each temperature are able to correct the interactions between different molecules that influence the liquid density property. Thus, we can state that the model accurately represents the experimental density data from a quantitative perspective. Experimental density values were fitted to a second-degree polynomial equation in T (Eq. (15)). The fitting parameters are applied to each temperature for calculation of AAD (%). The value is found to be 0.12 %. The second-degree polynomial equation in T better explains the interactions in ChCl/PA DES + 1-butanol binary mixtures. Figs. 11 and 12 show the variation of density with temperature (axis x) and with the mole fraction of des (axis x), respectively. According to Fig. 11, it is generally observed that, given the mole fraction of DES, the experimental density varies linearly with temperature. Similarly, the PC-SAFT model also shows a linear variation of density with temperature across all mole fractions of DES. Fig. 12 shows that PC-SAFT EoS correctly represents the experimental data of the density versus mole fraction of DES at a given temperature. Therefore, a good quantitative and

Table 10 Viscosity deviation $\Delta \eta$ of ChCl/PA DES + 1-butanol binary mixtures as a function of ChCl/PA DES mole fraction, x_1 , in the temperature range 293.15 \leq T/K \leq 333.15.

x ₁ /T(K)	$\Delta \eta/\text{mPa.s}$								
	293.15	298.15	303.15	308.15	313.15	318.15	323.15	328.15	333.15
0.00	0	0	0	0	0	0	0	0	0
0.10	-4.544	-3.655	-2.844	-2.262	-1.795	-1.460	-1.186	-0.988	-0.769
0.20	-9.224	-7.306	-5.605	-4.355	-3.394	-2.708	-2.161	-1.758	-1.353
0.30	-13.86	-10.97	-8.494	-6.660	-5.242	-4.134	-3.326	-2.699	-2.078
0.40	-18.43	-14.51	-11.17	-8.685	-6.842	-5.425	-4.320	-3.479	-2.716
0.50	-22.84	-17.91	-13.71	-10.70	-8.397	-6.608	-5.280	-4.268	-3.328
0.60	-24.64	-19.98	-15.86	-12.75	-10.09	-7.996	-6.397	-5.266	-4.146
0.70	-24.64	-19.73	-15.49	-12.38	-10.04	-8.252	-6.951	-5.977	-4.780
0.80	-20.62	-16.85	-12.88	-10.43	-7.917	-6.598	-5.491	-4.885	-3.986
0.90	-13.48	-11.16	-8.633	-6.795	-5.270	-4.080	-3.596	-3.329	-2.925
1.00	0	0	0	0	0	0	0	0	0

Standard uncertainties, u, in T, x, P and η are u(T)=0.02 (for viscosity) K, $u(x_1)=0.01$, u(p)=10kPa and $u(\Delta\eta)=0.1$ mPa.S.

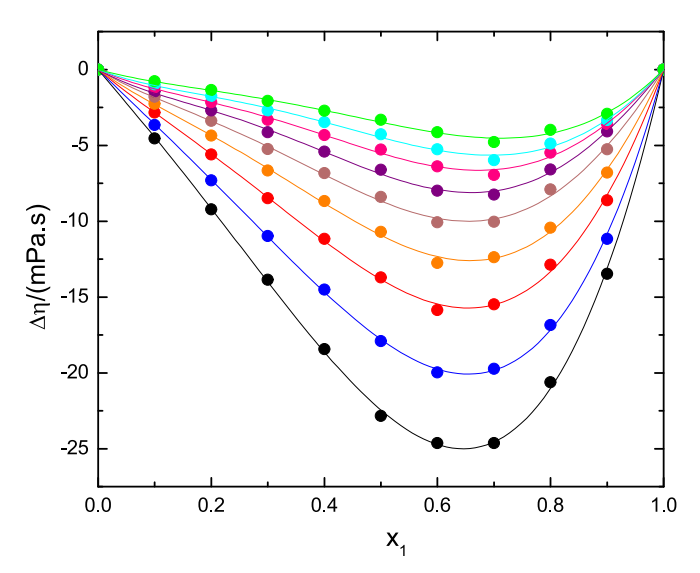


Fig. 10. Viscosity Deviation, $\Delta \eta$ of ChCl/PA DES + 1-butanol binary mixtures as a function of x_1 in the temperature range $293.15 \le T/K \le 333.15 \bullet (black)$: $293.15 \text{ K}; \bullet (blue)$: $298.15 \text{ K}; \bullet (red)$: $303.15 \text{ K}; \bullet (orange)$: $308.15; \bullet (brown)$: $313.15 \text{ K}; \bullet (purple)$: $318.15 \text{ K}; \bullet (pink)$: $323.15 \text{ K}; \bullet (cyan)$: $328.15 \text{ K}; \bullet (green)$: 333.15 K). The solid lines are the best fit representation of Eq. (21).

Table 11Parameters for pure fluids required in PC-SAFT EoS.

Fluid	m	$\sigma/(ext{Å})$	$\varepsilon/k_B/({ m K})$	$arepsilon^{AB}/k_B/({ m K})$	κ^{AB}
1-butanol [87]	3.5755	3.2646	227.19	2296.37	0.01765
DES	5.19041	2.97728	363.92	5943.82	0.18824

qualitative agreement is observed between experimental and theoretical data. This means that London dispersion forces and hydrogen bond forces between DES and 1-butanol are well modeled for an adequate representation of the density of these pseudo binary mixtures.

Regarding the modeling of the speed of sound, the liquid density data used in the speed of sound equations for both models (SCFT and NR) were obtained from the PC-SAFT EoS. The absolute average deviations were 8.87 % and 4.19 % using SCFT and NR models. According to these results, NR + PC-SAFT correctly predicts the speed of sound from a quantitative point of view.

Figs. 13 and 14 show the variation of speed of sound with temperature (axis x) and with the mole fraction of des (axis x), respectively. Based on Fig. 13, it is evident that the theoretical data from the NR

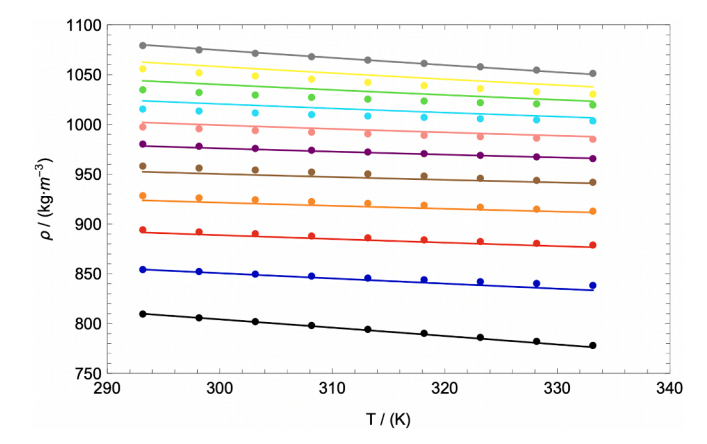


Fig. 11. Variation of density with temperature for the ChCl/PA DES + 1 butanol mixture at 0.1 MPa and different mole fractions of ChCl/PA DES. $x_1 = (\bullet(\text{black}); 0.0; \bullet(\text{blue}); 0.1; \bullet(\text{red}); 0.2; \bullet(\text{orange}); 0.3; \bullet(\text{brown}); 0.4; \bullet(\text{purple}); 0.5; \bullet(\text{pink}); 0.6; \bullet(\text{cyan}); 0.7; \bullet(\text{green}); 0.8; \bullet(\text{yellow}); 0.9; \bullet(\text{gray}); 1.0). Lines represents the theoretical results with PC-SAFT EoS and <math>k_{ij} = 0.695017 - 0.00287885 \bullet \text{T/K}$.

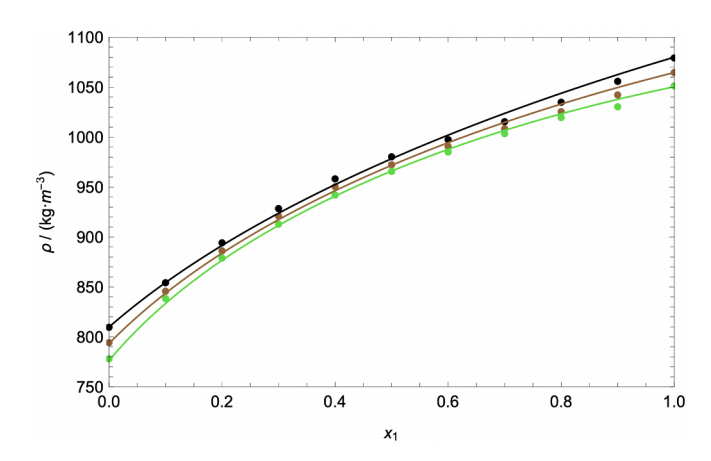


Fig. 12. Variation of density with mole fraction of DES for the ChCl/PA DES + 1 butanol mixture at 0.1 MPa and different temperatures of ChCl/PA DES (\bullet (black): 293.15 K; \bullet (brown): 313.15 K; \bullet (green): 333.15 K). Lines represents the theoretical results with PC-SAFT EoS and $k_{ij}=0.695017-0.00287885 \bullet T/K$.

model coincide with the experimental data at $x_1=0.0$ (1-butanol pure) and $x_1=1.0$ (DES pseudo pure), because NR model does not model the speed of sound for pure fluids. Instead, it uses the experimental values of pure fluids to predict this property in mixtures. Additionally, it is observed that the speed of sound decreases with increasing temperature and rises as the amount of DES in the mixture increases.

Fig. 14 illustrates the variation of the speed of sound with the mole fraction of des for three temperatures (293.15 K, 313.15 K, and 323.15 K). The dependence of the speed of sound on mole fraction and temperature is well represented by this model. On the other hand, from Figs. 13 and 14, the NR model exhibits a solid qualitative alignment with the experimental data. Additionally, it accurately represents the influence of intermolecular interactions in this property (both qualitatively and quantitatively), within the analyzed range of mole fractions and temperatures.

Finally, with respect to the FVT model + PC-SAFT, it can be applied to pure fluid mixtures and binary mixtures. The fitted parameters of FVT are fitted using the objective function defined as the mean absolute deviation of viscosity. The fitted parameters obtained for the DES are $\alpha=68527.70~\rm J\cdot mol^{-1},~B=0.143672,~l=1.029905~\rm x10^{-11}$ m, while for the 1-butanol are $\alpha=76769.28~\rm J\cdot mol^{-1},~B=0.0750461,~l=1~\rm x\,10^{-11}$ m. The deviations obtained with these parameters are 1.36 % and 2.14 % for DES and 1-butanol, respectively.

Therefore, FVT + PC-SAFT is able to appropriately model the experimental data of the viscosity of DES and 1-butanol fluids. Regarding the modeling of the experimental viscosity of the mixture, the parameters l_{ij} , w_{ij} , and u_{ij} are optimized using the mean absolute deviation (considering all temperatures and mole fractions) and the following optimal parameters are obtained: $l_{ij} = -0.213576$, $w_{ij} = 0.835147$, and $u_{ij} = -3.060214$, and the absolute average deviation was 10.85 %. So, according to our results, a high deviation is obtained for the viscosity of the mixture, however, it would be beneficial to study the qualitative modeling of this property. This deviation could be reduced by using fitted parameters specific to each temperature or by establishing a correlation between these parameters and temperature. However, we tested several temperature-dependent correlations and found no clear relationship with temperature that noticeably improved the representation of the experimental data.

Figs. 15 and 16 illustrate the variation of viscosity with temperature (axis x) and with the mole fraction of DES (axis x), respectively. From Fig. 15 it is observed that for pure DES and pure 1-butanol, the viscosity

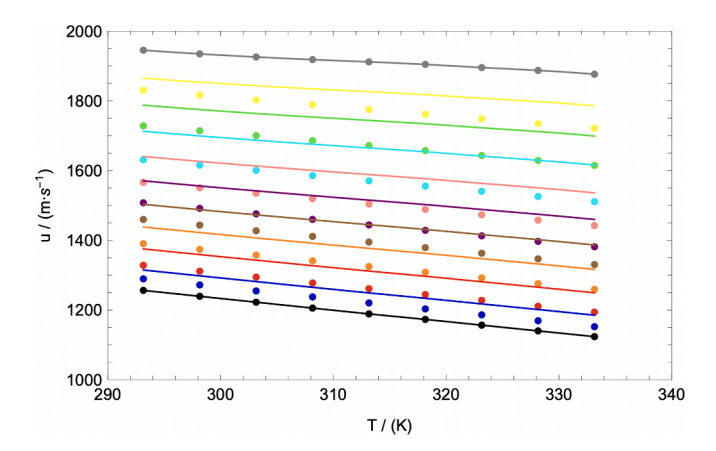


Fig. 13. Variation of speed of sound with temperature for the ChCl/PA DES +1 butanol mixture at 0.1 MPa and different mole fractions of ChCl/PA DES $x_1 = (\bullet(black): 0.0; \bullet(blue): 0.1; \bullet(red): 0.2; \bullet(orange): 0.3; \bullet(brown): 0.4; \bullet(purple): 0.5; \bullet(pink): 0.6; \bullet(cyan): 0.7; \bullet(green): 0.8; \bullet(yellow): 0.9; \bullet(gray): 1.0). Lines represents the theoretical results with NR + PC-SAFT EoS and <math>k_{ij} = 0.695017 - 0.00287885 \bullet T/K$.

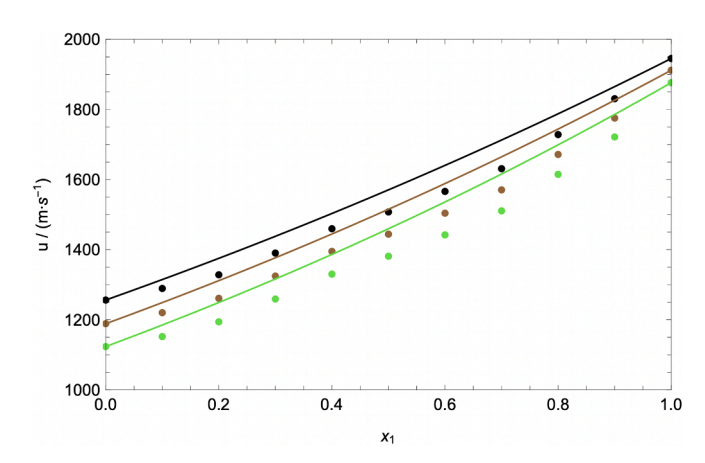


Fig. 14. Variation of speed of sound with mole fraction of DES for the ChCl/PA DES + 1 butanol mixture at 0.1 MPa and different temperatures of ChCl/PA DES (\bullet (black): 293.15 K; \bullet (brown): 313.15 K; \bullet (green): 333.15 K). Lines represents the theoretical results with NR + PC-SAFT EoS and $k_{ij}=0.695017-0.00287885 <math>\bullet$ T/K.

is modeled correctly, which is consistent with the deviations of 1.36 % and 2.14 % for DES and 1-butanol, respectively. Furthermore, it is anticipated that the non-linear variation of viscosity with temperature is modeled very well at least as a qualitative approach.

On the other hand, in Fig. 16 the variation of viscosity with the DES molar fraction is correctly modeled from a qualitative point of view (as described above). According to the figures above, it is accomplished that the resistance to flow of these binary mixture increases with the amount of DES in the mixture and with decreasing temperature (cohesive forces become weaker).

4. Conclusion

Deep eutectic solvent formed by interacting choline chloride (ChCl) and propionic acid (PA) in 1:2 mol ratio is reported. Density, speed of sound and dynamic viscosity of the deep eutectic solvent, ChCl/PA DES, and its binary mixtures with 1-butanol have been measured at T = (293.15 - 333.15)K in the entire range of composition. The experimental density data is fitted to a second-degree polynomial equation in T (correlation factor $r^2\,{=}\,0.999)$ and fourth degree polynomial equation in x_1 (r² = 0.999). Properties of the neat ChCl/PA DES, such as molecular volume V, standard entropy S^0 , and lattice energy U_{pot} , are evaluated from the experimental density data. Excess properties, V^E , $\Delta \kappa_S$ and $\Delta \eta$, of ChCl/PA DES + 1-butanol solutions are calculated over the entire composition and T = (293.15 - 333.15)K range and fitted with Redlich-Kister polynomial equation. The minima in V^E and $\Delta \kappa_S vs x_1$ plots occur at $x_1 \approx 0.35$ which lie in the 1-butanol rich region. The negative V^E values are attributed to the presence of specific interactions or dominant packing effect between the components of the mixtures. It explains the strong hydrogen bonding between the components of mixtures (ChCl/ PA DES and 1-butanol). As compared to V^E and $\Delta \kappa_S$, the minimum in the $\Delta \eta v s x_1$ plots of binary mixtures (ChCl/PA DES + 1-butanol) are shifted to $x_1 \approx 0.65$ which lies in the ChCl/PA DES rich region. Similar behavior is normally observed when deviations are compared as a function of composition and are mutually supportive. The calculated AAD for derived properties V^E , $\Delta \kappa_S$ and $\Delta \eta$ are 0.023 m³. mol⁻¹, 0.05 Pa⁻¹ and 0.1 mPa-s, respectively. The temperature dependance of transport property (η) are correlated with Vogel-Fulcher-Tammann (VFT) and Arrhenius models and compared. The VFT equation satisfactorily describes the variation of η with T.

The assumption of DES as a pure fluid and that DES with 1-butanol forms a binary mixture allowed to obtain in a simplified way (with the use of PC-SAFT and other models) good qualitative results for all properties. For liquid density, the deviation is 0.41 %, while for speed of

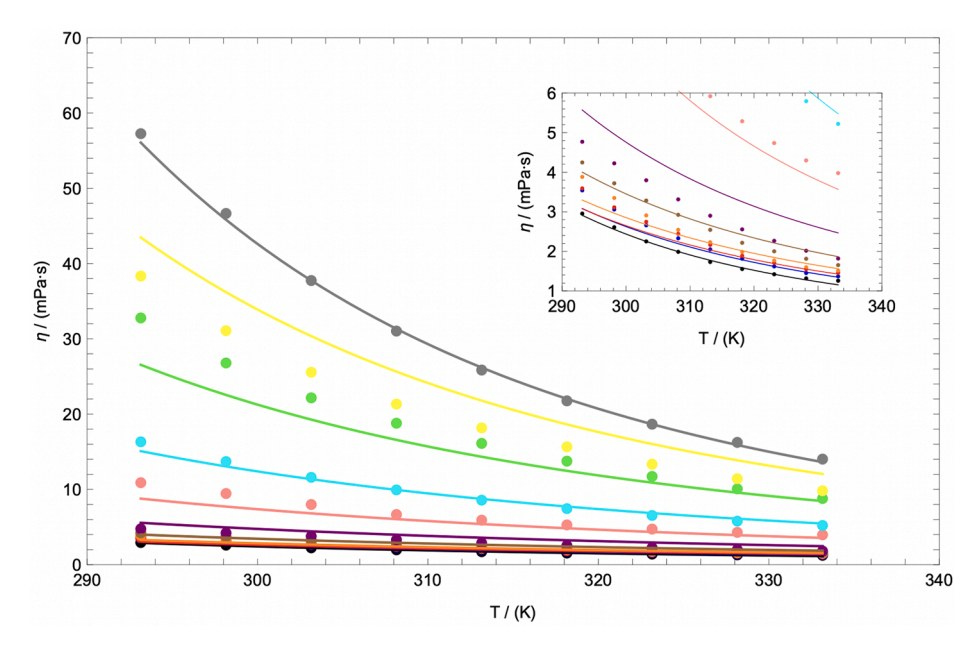


Fig. 15. Variation of viscosity with temperature for the ChCl/PA DES +1 butanol mixture at 0.1 MPa and different mole fractions of ChCl/PA DES $x_1 = (\bullet(\text{black}): 0.0; \bullet(\text{blue}): 0.1; \bullet(\text{red}): 0.2; \bullet(\text{orange}): 0.3; \bullet(\text{brown}): 0.4; \bullet(\text{purple}): 0.5; \bullet(\text{pink}): 0.6; \bullet(\text{cyan}): 0.7; \bullet(\text{green}): 0.8; \bullet(\text{yellow}): 0.9; \bullet(\text{gray}): 1.0). Lines represents the theoretical results with FVT <math>+$ PC-SAFT EoS, $k_{ij} = 0.695017 - 0.00287885 \bullet T/K$, and $l_{ij} = -0.213576$, $w_{ij} = 0.835147$, and $u_{ij} = -3.060214$.

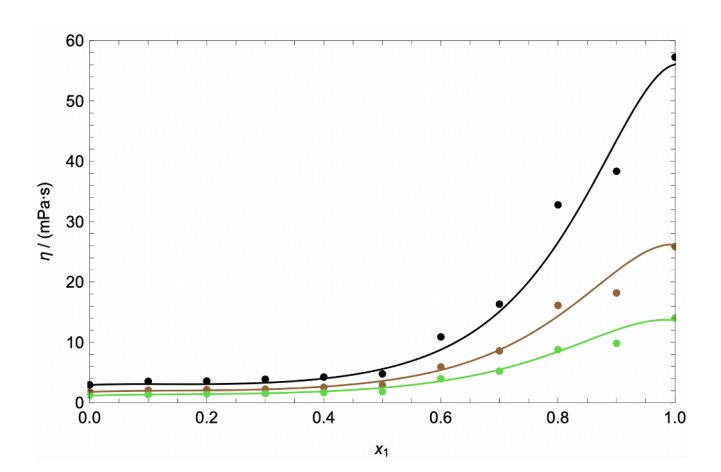


Fig. 16. Variation of viscosity with mole fraction of DES for the ChCl/PA DES + 1 butanol mixture at 0.1 MPa and different temperatures of ChCl/PA DES (\bullet (black): 293.15 K; \bullet (brown): 313.15 K; \bullet (green): 333.15 K). Lines represents the theoretical results with FVT + PC-SAFT EoS, $k_{ij}=0.695017-0.00287885 <math>\bullet$ T/K, and $l_{ij}=-0.213576$, $w_{ij}=0.835147$, and $u_{ij}=-3.060214$.

sound with NR + PC-SAFT and viscosity with FVT + PC-SAFT were 4.19 % and 10.85 %, respectively, which indicates a good quantitative agreement for density and speed of sound in the range of molar fraction and temperature range studied. Finally, the instantaneous dipole – induced dipole and hydrogen bond intermolecular interactions (considering Scheme 2B for both fluids), are correctly represented at least qualitatively for all properties.

CRediT authorship contribution statement

Aafia Sheikh: Writing – original draft, Methodology, Investigation,

Data curation, Conceptualization. **Ariel Hernández:** Writing – review & editing, Validation, Software, Investigation, Formal analysis. **Athar Yaseen Khan:** Writing – review & editing, Validation, Supervision, Resources, Project administration. **Safeer Ahmed:** Software, Formal analysis.

Declaration of competing interest

The authors declare that they have no known competing financial interests or personal relationships that could have appeared to influence the work reported in this paper.

Acknowledgements

The authors are thankful to Department of chemistry, Forman Christian College (A chartered University) Lahore, Pakistan on providing technical support.

Appendix A. Supplementary material

Supplementary data to this article can be found online at https://doi.org/10.1016/j.molliq.2025.127217.

Data availability

Data will be made available on request.

References

- P. Han, W. Nie, G. Zhao, P. Gao, Theoretical investigation on the structure and physicochemical properties of choline chloride-based deep eutectic solvents, J. Mol. Liq. 366 (2022) 120243.
- P. Wassercheid, T. Welton, Ionic Liquids in Synthesis, second edition, John Wiley, 2007.
- [3] J.B. Harper, M.N. Kobrak, Understanding organic processes in ionic liquids: achievements so far and challenges remaining, Mini Rev. Org. Chem. 3 (2006) 253–269.

- [4] K. Biernacki, H.K.S. Souza, C.M.R. Almeida, A.L. Magalhães, M.P. Gonçalves, Physicochemical properties of choline chloride-based deep eutectic solvents with polyols: an experimental and theoretical invewstigation, ACS Sustain. Chem. Eng. 8 (2020) 18712–18728.
- [5] E.L. Smith, A.P. Abbot, K.S. Ryder, Deep eutectic solvents (DESs) and their applications, Chem. Rev. 114 (2014) 11060–11082.
- [6] A. Mero, S. Koutsoumpos, P. Giannios, I. Stavrakas, K. Moutzouris, A. Mezzetta, L. Guazzelli, Comparison of physicochemical and thermal properties of choline chloride and betaine-based deep eutectic solvents: the influence of hydrogen bond acceptor and hydrogen bond donor nature and their molar ratios, J. Mol. Liq. 377 (2023) 121563.
- [7] S. Verma, K. Saini, S. Maken, Deep eutectic solvents: a long-term approach to chemical synthesis and separation, J. Mol. Liquids 393 (2024) 123605.
- [8] M. Hayyan, M.A. Hashim, A. Hayyan, M.A. Al-Saadi, I.M. AlNashef, M.E. S. Mirghani, O.K. Saheed, Are deep eutectic solvents benign or toxic? Chemosphere 90 (2013) 2193–2195.
- [9] D. Zhao, Y. Liao, Z. Zhang, Toxicity of ionic liquids, Clean–Soil Air Water. 35 (2007) 42–48.
- [10] S. Gahlyan, M. Rani, S. Maken, H. Kwon, K. Tak, I. Moon, Modeling of thermodynamic properties of an oxygenate + aromatic hydrocarbon: excess molar enthalpy, J. Ind. Eng. Chem. 23 (2015) 299–306.
- [11] K. Radošević, M. Cvjetko Bubalo, V. Gaurina Srček, D. Grgas, T. Landeka Dragičević, I. Radojčić Redovniković, Evaluation of toxicity and biodegradability of choline chloride based deep eutectic solvents, Ecotoxicol. Environ. Saf. 112 (2015) 46–53.
- [12] D.O. Abranches, L.P. Silva, M.A.R. Martins, S.P. Pinho, J.A.P. Coutinho, Understanding the formation of deep eutectic solvents: betaine as a universal hydrogen bond acceptor, ChemSusChem 13 (2020) 4916–4921.
- [13] A. Sheikh, A.Y. Khan, S. Ahmed, Physicochemical properties of choline chloride/ acetic acid as a deep eutectic solvent and its binary solutions with DMSO at 298.15 to 353.15 K, ACS Omega 9 (2024) 3730–3745.
- [14] M. Khorsandi, H. Shekaari, M. Mokhtarpour, Measurement and correlation of coumarin solubility in aqueous solution of acidic deep eutectic solvents based on choline chloride, Fluid Phase Equilib. 524 (2020) 112788.
- [15] X. Kang, C. Deng, R. Shinde, R. Lin, J.D. Murphy, Renewable deep eutectic solvents pretreatment improved the efficiency of anaerobic digestion by lignin extraction from willow, Energy Convers. Manag. 288 (2023) 117115.
- [16] D. Shah, F.S. Mjalli, Effect of water on the thermo-physical properties of Reline: an experimental and molecular simulation-based approach, Phys. Chem. Chem. Phys. 16 (2014) 23900–23907.
- [17] M.M. Nolasco, S.N. Pedro, C. Vilela, P.D. Vaz, P. Ribeiro-Claro, S. Rudic, S. F. Parker, C.S.R. Freire, M.G. Friere, A.J.D. Silvestre, Water in deep eutectic solvents: new insights from inelastic neutron scattering spectroscopy, Front. Phys. 10 (2022) 834571.
- [18] H. Passos, D.J.P. Tavares, A.M. Ferreira, M.G. Freire, J.A.P. Coutinho, Are aqueous biphasic systems composed of deep eutectic solvents ternary or quaternary systems? ACS Sustain. Chem. Eng. 4 (2016) 2881–2886.
- [19] A. Sheikh, I. Saleem, S. Ahmed, M. Abbas, A.Y. Khan, Investigation of physicochemical properties of NADES based on choline chloride and ascorbic acid and its binary solutions with DMSO from (298.15 to 353.15) K, J. Mol. Liq. 364 (2022) 120038.
- [20] Y. Chen, D. Yu, W. Chen, L. Fu, T. Mu, Water absorption by deep eutectic solvents, Phys. Chem. Chem. Phys. 21 (2019) 2601–2610.
 [21] A. Shishov, A. Bulatov, M. Locatelli, S. Carradori, V. Andruch, Application of deep
- [21] A. Shishov, A. Bulatov, M. Locatelli, S. Carradori, V. Andruch, Application of deep eutectic solvents in analytical chemistry. A review, Microchem. J. 135 (2017) 33–38
- [22] C. Florindo, L.C. Branco, I.M. Marrucho, Quest for green-solvent design: from hydrophilic to hydrophobic (Deep) eutectic solvents, ChemSusChem 12 (2019) 1549–1559.
- [23] A.K. Jangir, B. Lad, U. Dani, N. Shah, K. Kuperkar, *In vitro* toxicity assessment and enhanced drug solubility profile of green deep eutectic solvent derivatives (DESDs) combined with theoretical validation, RSC Adv. 10 (2020) 24063–24072.
- [24] V. Viera, M.A. Prieto, L. Barros, J.A.P. Coutinho, I.C.F.R. Ferreira, O. Ferreira, Enhanced extraction of phenolic compounds using choline chloride based deep eutectic solvents from *Juglans regia* L. Ind. Crop Prod. 115 (2018) 261–271.
- [25] K.H. Almashjary, M. Khalid, S. Dharaskar, P. Jgadish, R. Walvekar, T.C.S.M. Gupta, Optimisation of extractive desulfurization using choline chloride-based deep eutectic solvents, Fuel 234 (2018) 1388–1400.
- [26] A.A. Alluhaybi, A.M. Hameed, M.T. Alotaibi, A. Alharbi, A. Shahat, Synthesis and characterization of carbon nanospheres for adsorption of ibuprofen from aqueous solution: optimization by Box–Behnken design, J. Mol. Liq. 383 (2023) 122059.
- [27] M. Li, C. Zhu, T. Fu, X. Gao, Y. Ma, Effect of water on amine-based deep eutectic solvents (choline chloride + monoethanolamine): structure and physicochemical properties, J. Environ. Chem. Eng. 1 (2023) 106952.
- [28] A. García, E. Rodríguez-Juan, G. Rodríguez-Gutiérrez, J.J. Rios, J. Fernández-Bolaños, Extraction of phenolic compounds from virgin olive oil by deep eutectic solvents (DESs), Food Chem. 197 (2016) 554–561.
- [29] N.F. Gajardo-Parra, M.J. Lubben, J.M. Winnert, Á. Leiva, J.F. Bennecke, R. I. Canales, Physicochemical properties of choline chloride-based deep eutectic solvents and excess properties of their pseudo-binary mixtures with 1-butanol, J. Chem. Thermodyn. 133 (2019) 272–284.
- [30] J. Potvin, P. Péringer, Influence of n-propanol on growth and antibiotic production by an industrial strain of streptomyces erythreus under different nutritional conditions, Biotechnol. Lett 15 (1993) 455–460.
- [31] L. Sun, C.D. WickJ, I. Siepmann, M.R. Schure, Temperature dependence of hydrogen bonding: an investigation of the retention of primary and secondary

- alcohols in gas–liquid chromatography, J. Phys. Chem. B 105 (2009) 15118-15125.
- [32] M.L. Rotter, W. Koller, R. Neumann, The influence of cosmetic additives on the acceptability of alcohol-based hand disinfectants, J. Hosp. Infect. 18 (1991) 57–63.
- [33] F. Merza, A. Fawzy, I. AlNashef, S. Al-Zuhair, H. Taher, Effectiveness of using deep eutectic solvents as an alternative to conventional solvents in enzymatic biodiesel production from waste oils, Energy Rep. 4 (2018) 77–83.
- [34] K. Mamtani, K. Shahbaz, M.M. Farid, Deep eutectic solvents Versatile chemicals in biodiesel production, Fuel 295 (2021) 120604.
- [35] J. Safarov, B. Ahmadov, S. Mirzayev, A. Shahverdiyev, E.P. Hassel, Thermophysical properties of 1-butanol over a wide range of temperatures and pressures up to 200 MPa, J. Mol. Liq. 209 (2015) 465–479.
- [36] M. Dzida, Thermophysical properties of 1-butanol at high pressures, Energies 13 (2020) 5046.
- [37] S. Atsumi, T. Hanai, J.C. Liao, Non-fermentative pathways for synthesis of branched chain higher alcohols as biofuels, Nature 451 (2008) 86–89.
- [38] S. Verma, S. Kim, S. Maken, Y. Lee, Experimental and theoretical studies of binary liquid mixtures containing methyl 2-hydroxyisobutyrate and alkanol (C₃-C₄) at 288.15 K-323.15 K, J. Chem. Thermodyn. 195 (2024) 107291.
- [39] S. Verma, S. Gahlyan, P. Bhagat, M. Rani, S. Rana, Y. Lee, S. Maken, Transport and optical properties of n-butylamine + alkanols (C₃-C₄) mixtures for enhanced CO₂ absorption, Korean J. Chem. Eng. 41 (2024) 715–727.
- [40] A.K. Jangir, D. Patel, R. More, A. Parmer, K. Kuperkar, New insight into experimental and computational studies of Choline chloride-based 'green' ternary deep eutectic solvent (TDES), J. Mol. Struct. 1181 (2019) 295–299.
- [41] N.F. Gajardo-Parra, V.P. Cotreno-Figueroa, P. Arvena, V. Vesovic, R.I. Canalis, Viscosity of choline chloride-based deep eutectic solvents: experiments and modeling, J. Chem. Eng. Data 65 (2020) 5581–5592.
- [42] J. Gross, G. Sadowski, Perturbed-chain SAFT, an equation of state based on a perturbation theory for chain molecules, Ind. Eng. Chem. Res. 40 (2001) 1244–1260
- [43] J. Gross, G. Sadowski, Application of the perturbed-chain SAFT equation of state to associating systems, Ind. Eng. Chem. Res. 41 (2002) 5510–5515.
- [44] W. Schaaffs, The problem of a theoretical calculation of the velocity of sound for binary liquid mixtures, Acta Acust. Acust. 33 (1975) 272–276.
- [45] O. Nomoto, Empirical formula for sound velocity in liquid mixtures, J. Phys. Soc. Jpn. 13 (1958) 1528–1532.
- [46] A. Allal, C. Boned, P. Daugé, A new free volume model for dynamic viscosity of dense fluids versus pressure and temperature. Extension to a predictive model for not very associative mixtures, Phys. Chem. Liq. 39 (2001) 607–624.
- [47] A. Allal, M. Moha-Ouchane, C. Boned, A new free volume model for dynamic viscosity and density of dense fluids versus pressure and temperature, Phys. Chem. Liq. 39 (2001) 1–30.
- [48] A. Allal, C. Boned, A. Baylaucq, Free-volume viscosity model for fluids in the dense and gaseous states, Phys. Rev. E 64 (2001) 011203.
- [49] W. Wang, M.M. Sabuga, S. Chandra, Y.P. Asmara, B.A. Alreda, N. Ulloa, Y. Almasry, M.M. Kadhim, Choline chloride-based deep eutectic solvents as electrolytes for wide temperature range supercapacitors, J. Energy Storage 71 (2023) 108141.
- [50] Y. Cui, C. Li, J. Yin, S. Li, Y. Jia, M. Bao, Design, synthesis and properties of acidic deep eutectic solvents based on choline chloride, J. Mol. Liq. 236 (2017) 338–343.
- [51] N. Mgxadeni, A. Hernández, I. Bahadur, F. Mohammad, A.A. Soleiman, Correlation and modelling the thermodynamics properties of mixtures containing zinc (II) chloride-based deep eutectic solvent and alkanols with PC-SAFT EoS, and the Nomoto's relation, J. Mol. Liq. 397 (2024) 124155.
- [52] N. Mgxadeni, B. Kabane, A. Hernández, I. Bahadur, F. Mohammad, A.A. Soleiman, M.M. Kabanda, Application of PC-SAFT EoS and SCFT for the modeling of thermophysical properties comprising deep eutectic solvent and alcohols, Asia-Pac. J. Chem. Eng. 2024 (2024).
- [53] V.P. Cotroneo-Figueroa, N.F. Gajardo-Parra, P. López-Porfiri, Á. Leiva, M. Gonzalez-Miquel, J.M. Garrido, R.I. Canales, Hydrogen bond donor and alcohol chain length effect on the physicochemical properties of choline chloride based deep eutectic solvents mixed with alcohols, J. Mol. Liq. 345 (2022) (2022) 116986.
- [54] E.A. Crespo, J.M. Costa, A.M. Palma, B. Soares, M.C. Martín, J.J. Segovia, J. A. Coutinho, Thermodynamic characterization of deep eutectic solvents at high pressures, Fluid Phase Equilib. 500 (2019) 112249.
- [55] T.H. Chung, M. Ajlan, L.L. Lee, K.E. Starling, Generalized multiparameter correlation for nonpolar and polar fluid transport properties, Ind. Eng. Chem. Res. 27 (1988) 671–679.
- [56] S.P. Ijardar, Deep eutectic solvents composed of tetrabutylammonium bromide and PEG: Density, speed of sound and viscosity as a function of temperature, J. Chem. Thermodyn. 140 (2020) 105897.
- [57] F. Chemat, H. Anjum, A.M. Shariff, P. Kumar, T. Murugesan, Thermal and physical properties of (Choline chloride + urea + L-arginine) deep eutectic solvents, J. Mol. Liq. 218 (2016) 301–308.
- [58] F. Kermanpour, Thermodynamic study of binary mixtures of propilophenone + 2-propanol, 2-butanol, 2-pentanol, or 2-hexanol at temperatures of 293.15 to 323.15 K: modeling by Prigogine-Flory-Patterson theory, J. Mol. Liq. 376 (2023) 121448.
- [59] Y. Zhao, C. Guo, Y. Li, J. Wang, J. Tong, Study on physicochemical and excess properties of [HEMIM][Ala] with DMSO/H₂O binary mixtures, J. Mol. Liq. 343 (2021) 117491.
- [60] L. Glasser, Lattice and phase transition thermodynamics of ionic liquids, Thermochim. Acta 421 (1–2) (2004) 87–93.
- [61] D.R. Lide, CRC Handbook of Chemistry and Physics, vol. 85, CRC Press, 2004.

- [62] Y. Shi, S. Liu, S. Wang, Y. Yu, X. Chen, X. Zhu, Thermodynamic properties of DBN-based ionic liquids and their binary mixtures with primary alcohols, J. Mol. Liq. 371 (2023) 121060.
- [63] K. Singh, R.P. Shibu, S. Mehra, A. Kumar, Insights into the physicochemical properties of newly synthesized benzyl triethylammonium chloride-based deep eutectic solvents, J. Mol. Liq. 386 (2023) 122589.
- [64] B. Nowosielski, M. Jamrógiewicz, J. Łuczak, M. Śmiechowski, D. Warmińska, Experimental and predicted physicochemical properties of monopropanolaminebased deep eutectic solvents, J. Mol. Liq. 309 (2020) 113110.
- [65] N. Chaudhary, A.K. Nain, Densities, speeds of sound, refractive indices, excess and partial molar properties of polyethylene glycol 200 + benzyl methacrylate binary mixtures at temperatures from 293.15 to 318.15 K, J. Mol. Liq. 343 (2022) 117923.
- [66] J.G. Parra, Y.R. Array, P. Iza, X. Zarate, E. Schott, Behavior of the SDS/1-butanol and SDS/2-butanol mixtures at the water/n-octane interface through molecular dynamics simulations, Chem. Phys. 523 (2019) 138–149.
- [67] L. de Villiers Engelbrecht, R. Farris, T. Vasiliu, M. Demurtas, A. Piras, F. C. Marincola, A. Laaksonen, S. Porcedda, F. Mocci, Theoretical and experimental study of the excess thermodynamic properties of highly nonideal liquid mixtures of butanol isomers + DBE, J. Phys. Chem. B 125 (2021) 587–600.
- [68] R. Haghbakhsh, S. Raeissi, Investigation of solutions of ethyl alcohol and the deep eutectic solvent of Reline for their volumetric properties, Fluid Phase Equilib. 472 (2018) 39-47
- [69] S.P. Šerbanović, M.L. Kijevčanin, I.R. Radović, B.D. Djordjević, Effect of temperature on the excess molar volumes of some alcohol + aromatic mixtures and modelling by cubic EOS mixing rules, Fluid Phase Equilib. 239 (2006) 69–82.
- [70] K.-S. Kim, B.H. Park, Volumetric properties of solutions of choline chloride + glycerol deep eutectic solvent with water methanol, ethanol, or iso-propanol, J. Mol. Liq. 254 (2018) 272–279.
- [71] O. Redlich, A.T. Kister, Thermodynamics of non-electrolyte solutions, x-y-t relation in binary system, Ind. Eng. Chem. 40 (1948) 341–345.
- [72] S. Verma, P. Kashyap, M. Rani, H. Song, S. Maken, Volumetric, acoustic, and optical properties of binary mixtures of diethyl ether with alkanol at T = 293.15 K to 303.15 K, J. Mol. Liq. 394 (2024) 123796.
- [73] D. Dragoescu, F. Sirbu, L. Almásy, Study of the thermophysical properties for aqueous alkanediols binary mixtures, J. Mol. Liq. 335 (2018) 272–279.
- [74] M. Dzida, E. Zorębski, M. Zorębski, M. Zarska, M.-G. Rybczyńska, M. Chorążewski, J. Yacquemin, I. Cibulka, Speed of sound and ultrasound absorption in ionic liquids, Chem. Rev. 117 (2017) 3883–3929.
- [75] M.I. Davis, G. Douheret, J.C.R. Reis, M.J. Blandamer, Apparent and partial ideal molar isentropic compressibilities of binary liquid mixtures, Phys. Chem. Chem. Phys. 3 (2001) 4555–4559.

- [76] T. Swebocki, A. Barras, A. Abderrahmani, K. Haddadi, R. Boukherroub, Deep eutectic solvents comprising organic acids and their application in (bio)medicine, Int. J. Mol. Sci. 24 (2023) 8492.
- [77] B. Jacobson, Ultrasonic velocity in liquids and liquid mixtures, J. Chem. Phys. 20 (1952) 927–928.
- [78] M.K. Praharaj, A. Satapathy, P. Mishra, S. Mishra, Ultrasonic studies of ternary liquid mixtures of N-N-dimethylformamide, nitrobenzene, and cyclohexane at different frequencies at 318 K, J. Theor. Appl. Phys. 23 (2013) 7–23.
- [79] U. Fatima, Riyazuddeen, N. Anwar, H. Campos, L.M. Varela, Molecular dynamic simulation, molecular interactions and structural properties of 1-butyl-3-methylimidazolium bis(trifluoromethylsulfonyl)imide b 1-butanol/1-propanol mixtures at (298.15-323.15) K and 0.1 M Pa, Fluid Phase Equillib. 472 (2018) 9–21.
- [80] H. Ghaedi, M. Ayoub, S. Sufian, A.M. Shariff, B. Lal, The study on temperature dependence of viscosity and surface tension of several Phosphonium-based deep eutectic solvents, J. Mol. Liq. 241 (2017) 500–510.
- [81] Q. Zheng, J.C. Mauro, Viscosity of glass-forming systems, J. Am. Ceram. Soc. 100 (2017) 6–25.
- [82] M. Peleg, Temperature–viscosity models reassessed, Crit. Rev. Food Sci. Nutr. 15 (2018) 2663–2672.
- [83] M. Peleg, M.D. Normand, M.G. Corradini, The Arrhenius equation revisited, Crit. Rev. Food Sci. Nutr. 52 (2012) 830–851.
- [84] R. Haghbakhsh, A.R.C. Duarte, S. Raeissi, Aqueous mixture viscosities of phenolic deep eutectic solvents, Fluid Phase Equilib. 553 (2022) 113290.
- [85] O.G. Sas, R. Fidalgo, I. Domínguez, E.A. Macedo, B. Gonzalez, Physical properties of the pure deep eutectic solvent, [ChCl]:[Lev] (1:2) DES, and its binary mixtures with alcohols, J. Chem. Eng. Data 61 (2016) 4191–4202.
- [86] P. Kaur, G.P. Dubey, Molecular interactions in 2-isopropoxy ethanol + alcohols: a thermo-physical and spectroscopic approach, J. Mol. Liq. 218 (2016) 246–254.
- [87] A. Hernández, M. Cartes, A. Mejía, The use of the PC-SAFT for modeling selected experimental thermophysical properties of dimethyl carbonate + 1-butanol binary mixture, J. Chem. Eng. Data 69 (2023) 639–649.
- [88] M. Moghimi, A. Roosta, Physical properties of aqueous mixtures of (choline chloride+ glucose) deep eutectic solvents, J. Chem. Thermodyn. 129 (2019) 159-165
- [89] S. Gholami, A. Roosta, Experimental study and modeling of bubble point of aqueous mixtures of deep eutectic solvents based on dicarboxylic acids and choline chloride, J. Chem. Eng. Data 65 (2020) 2743–2750.
- [90] S. Gholami, A. Roosta, Bubble point of aqueous mixtures of sugar-based deep eutectic solvents and their individual components: experimental study and modeling, J. Mol. Liquids 296 (2019) 111876.
- [91] L.F. Zubeir, C. Held, G. Sadowski, M.C. Kroon, PC-SAFT modeling of CO2 solubilities in deep eutectic solvents, J. Phys. Chem. B 120 (2016) 2300–2310.